JGP Journal of General Physiology

ARTICLE

Determinants of Ca^{2+} release restitution: Insights from genetically altered animals and mathematical modeling

Alejandra Cely-Ortiz[1]*, Juan I. Felice[1]*, Leandro A. Díaz-Zegarra[1], Carlos A. Valverde[1], Marilén Federico[1], Julieta Palomeque[1], Xander H.T. Wehrens[2], Evangelia G. Kranias[3], Ernesto A. Aiello[1], Elena C. Lascano[4], Jorge A. Negroni[4a], and Alicia Mattiazzi[1b]

Each heartbeat is followed by a refractory period. Recovery from refractoriness is known as Ca^{2+} release restitution (CRR), and its alterations are potential triggers of Ca^{2+} arrhythmias. Although the control of CRR has been associated with SR Ca^{2+} load and RYR2 Ca^{2+} sensitivity, the relative role of some of the determinants of CRR remains largely undefined. An intriguing point, difficult to dissect and previously neglected, is the possible independent effect of SR Ca^{2+} content versus the velocity of SR Ca^{2+} refilling on CRR. To assess these interrogations, we used isolated myocytes with phospholamban (PLN) ablation (PLNKO), knock-in mice with pseudoconstitutive CaMKII phosphorylation of RYR2 S2814 (S2814D), S2814D crossed with PLNKO mice (SDKO), and a previously validated human cardiac myocyte model. Restitution of cytosolic Ca^{2+} (Fura-2 AM) and L-type calcium current (ICaL; patch-clamp) was evaluated with a two-pulse (S_1/S_2) protocol. CRR and ICaL restitution increased as a function of the (S_2-S_1) coupling interval, following an exponential curve. When SR Ca^{2+} load was increased by increasing extracellular [Ca^{2+}] from 2.0 to 4.0 mM, CRR and ICaL restitution were enhanced, suggesting that ICaL restitution may contribute to the faster CRR observed at 4.0 mM [Ca^{2+}]. In contrast, ICaL restitution did not differ among the different mouse models. For a given SR Ca^{2+} load, CRR was accelerated in S2814D myocytes versus WT, but not in PLNKO and SDKO myocytes versus WT and S2814D, respectively. The model mimics all experimental data. Moreover, when the PLN ablation-induced decrease in RYR2 expression was corrected, the model revealed that CRR was accelerated in PLNKO and SDKO versus WT and S2814D myocytes, consistent with the enhanced velocity of refilling, SR [Ca^{2+}] recovery, and CRR. We speculate that refilling rate might enhance CRR independently of SR Ca^{2+} load.

Introduction

With each heartbeat, Ca^{2+} enters the cell through voltage-gated L-type Ca^{2+} channels to trigger Ca^{2+} release from the SR via CICR (Fabiato and Fabiato, 1977). Ca^{2+} released from the SR activates the myofilaments that drive contraction. Relaxation occurs when SR Ca^{2+} release is terminated, allowing the effective re-sequestration of cytosolic Ca^{2+} into the SR by SERCA2a and its extrusion from the cell by the Na^+/Ca^{2+} exchanger. This results in a decrease in cytosolic Ca^{2+}. After SR Ca^{2+} release, time must elapse before a second release event of equal amplitude can take place; that is, recovery of SR Ca^{2+} release must occur (DelPrincipe et al., 1999). This recovery from refractoriness is usually known as Ca^{2+} release restitution (CRR), which is a fundamental cellular property in determining beat-to-beat stability of CICR and hence is primarily involved in cardiac function and dysfunction. For instance, Ca^{2+} alternans, a gold standard example of beat-to-beat instability in cardiac myocytes, appears tightly associated with alterations in CRR (Hüser et al., 2000; Kornyeyev et al., 2012; Shkryl et al., 2012; Zhong et al., 2016; Sun et al., 2018). Moreover, CRR is significantly accelerated in postinfarction myocytes, thereby accounting for increased vulnerability of these myocytes to diastolic spontaneous arrhythmogenic Ca^{2+} waves and arrhythmias (Terentyev et al., 2002, 2003; Szentesi et al., 2004).

At the cellular level, several factors appear to affect refractoriness of SR Ca^{2+} release, including L-type Ca^{2+} current (ICaL), ryanodine receptors (RYR2) refractoriness and the mechanisms

[1]Centro de Investigaciones Cardiovasculares, Centro Científico Tecnológico–La Plata, Consejo Nacional de Investigaciones Científicas y Técnicas, Facultad de Ciencias Médicas, Universidad Nacional de La Plata, La Plata, Argentina; [2]Departments of Molecular Physiology and Biophysics, Medicine (in Cardiology), Neuroscience, Pediatrics, Center for Space Medicine, Baylor College of Medicine, Cardiovascular Research Institute, Houston, TX; [3]Department of Pharmacology, University of Cincinnati College of Medicine, Cincinnati, OH; [4]Instituto de Medicina Traslacional, Trasplante y Bioingeniería, Consejo Nacional de Investigaciones Científicas y Técnicas, Universidad Favaloro, Ciudad Autónoma de Buenos Aires, Buenos Aires, Argentina.

*A. Cely-Ortiz and J.I. Felice contributed equally to this paper; Correspondence to Jorge A. Negroni: negroni@favaloro.edu.ar; Alicia Mattiazzi: aliciamattiazzi@gmail.com.

© 2020 Cely-Ortiz et al. This article is distributed under the terms of an Attribution–Noncommercial–Share Alike–No Mirror Sites license for the first six months after the publication date (see http://www.rupress.org/terms/). After six months it is available under a Creative Commons License (Attribution–Noncommercial–Share Alike 4.0 International license, as described at https://creativecommons.org/licenses/by-nc-sa/4.0/).

Downloaded from http://rupress.org/jgp/article-pdf/152/11/e201912512/1801170/jgp_201912512.pdf by guest on 10 February 2026

involved in the regulation of SR Ca^{2+} load (Szentesi et al., 2004; Sobie et al., 2005; Ramay et al., 2011). However, and despite its physiological and clinical importance, the mechanisms underlying functional inactivation of Ca^{2+} release and the relative significance of CRR determinants remain not completely clear. Terentyev et al. (2008) concluded that calsequestrin plays a key role in CRR because it determines the "functional size and stability" of SR Ca^{2+} store. Other authors have shown that interventions which accelerate or slow SR refilling accelerate or slow CRR, respectively, independently of changes in cytosolic Ca^{2+} (Szentesi et al., 2004). Extending these previous findings, it has been shown that CRR depends not only on SR Ca^{2+} refilling but also on changes in RYR2 function itself, including the variations in Ca^{2+} sensitivity produced by mutations or post-translational modifications of the channel (Ramay et al., 2011; Zhong et al., 2016; Sun et al., 2018). Indeed, RYR2 refractoriness appears as a main factor in the determination of CRR and Ca^{2+} alternans (Picht et al., 2006; Belevych et al., 2012; Wang et al., 2014).

In previous studies, the relative role played by the velocity of SR Ca^{2+} refilling versus the level of SR Ca^{2+} load on CRR was not yet defined. Because the acceleration of SR Ca^{2+} refilling increases SR Ca^{2+} content, this intriguing aspect is difficult to dissect experimentally. However, the relative importance of these two factors on CRR might provide a clue to further clarify its underlying control mechanisms. If SR Ca^{2+} load, acting either directly on RYR2 (Jiang et al., 2007; Peng et al., 2016) or indirectly through the regulation of accessory luminal regulatory proteins (Pritchard and Kranias, 2009; Faggioni and Knollmann, 2012; Marty, 2015), contributes to the recovery of RYR2 from refractoriness, then the velocity of SR Ca^{2+} refilling might be of relevance. In contrast, if the recovery of Ca^{2+} release from refractoriness lags behind the recovery of SR Ca^{2+} load, as was demonstrated by Belevych et al. (2012), the velocity of SR Ca^{2+} refilling might not be a critical determinant of CRR.

In the present work, we combined experiments in genetically modified mice with mathematical modeling to examine the time course of CRR and dissect the different mechanisms involved in this recovery (i.e., RYR2 Ca^{2+} sensitivity, SR Ca^{2+} load, and the velocity of SR Ca^{2+} reuptake). We used mice with (1) phospholamban (PLN) ablation (PLNKO) to increase the velocity of SR Ca^{2+} reuptake and SR Ca^{2+} load, (2) knock-in mice with pseudoconstitutive phosphorylation of the Ser2814 Ca^{2+}/calmodulin-dependent protein kinase II (CaMKII) site on RYR2 (S2814D) exhibiting increased RYR2 Ca^{2+} sensitivity (Wehrens et al., 2004; van Oort et al., 2010), and (3) a cross of the PLNKO and S2814D mice (PLNKO×S2814D [SDKO]; Mazzocchi et al., 2016; Valverde et al., 2019) to produce acceleration of SR Ca^{2+} reuptake and increased RYR2 activity. The experimental conditions of the different models were recapitulated in a mathematical human myocyte model (Mazzocchi et al., 2016). The results indicated that SR Ca^{2+} load and RYR2 Ca^{2+} sensitivity are major determinants of CRR. Moreover, mathematical modeling led us to suggest that the velocity of SR Ca^{2+} refilling may play a role in CRR independently from that of SR Ca^{2+} content.

Materials and methods

Animals

Experiments were performed in 3–4-mo-old male mutant PLNKO mice (Luo et al., 1994), RYR2-S2814D$^{+/+}$ knock-in mice (S2814D; van Oort et al., 2010), and SDKO mice (Mazzocchi et al., 2016; Valverde et al., 2019). C57BL/6 mice, the genetic background of the different strains, were used as control animals (WT mice). Murine genotype was confirmed by PCR analysis using mouse tail DNA and specific primers for each mutation (Mazzocchi et al., 2016; Valverde et al., 2019). Animals were anesthetized with an intraperitoneal injection of ketamine–diazepam (100 mg/kg and 5 mg/kg, respectively). Central thoracotomy and heart excision were performed immediately after phase III anesthesia was reached, verified by the loss of pedal withdrawal reflex. All experiments involving mice were performed as per institutional guidelines and appropriate laws and were approved by the Faculty of Medicine, University of La Plata Institutional Animal Care and Use Committee (CICUAL no. T05-01-17).

Myocyte isolation

We used ventricular myocytes isolated from male mice in accordance with a modified protocol of Petroff et al. (2000). Briefly, the hearts were excised, cannulated in situ, and retrogradely perfused on a Langendorff system. Hearts were perfused at 37°C for 4 min with Tyrode solution containing EGTA (0.1 mM) and then immediately perfused for 7–9 min with a Ca^{2+}-free solution comprising (in mM): 140 NaCl, 4.69 KCl, 1.05 $MgSO_4$, 10 HEPES, 0.35 NaH_2PO_4, 11.1 glucose, and collagenase type 2 (0.5 mg/ml; Worthington Biochemical), pH 7.4. When hearts became flaccid (15–20 min), they were off-hook down, and myocytes were manually dissociated. After isolation, ventricular myocytes were slowly recalcified and kept at room temperature in a solution containing 1 mM Ca^{2+} until used.

Intracellular Ca^{2+} measurements

Isolated myocytes were loaded at room temperature with 5 µM Fura-2 acetoxymethyl ester (a cell-permeant form of Fura-2; Thermo Fischer Scientific) in Tyrode solution (HEPES buffered) containing 1 mM Ca^{2+} for 15 min. After being washed twice with 2 mM Ca^{2+} Tyrode solution, the cells were left for de-esterification for 30 min. Only rod-shaped myocytes with clear and distinct striations were used. Experiments were performed at room temperature (22–24°C) in Tyrode solution. The composition of the experimental Tyrode solution was as described above in the presence of 2 mM Ca^{2+} unless otherwise specified (pH 7.4; equilibrated with 100% O_2). The myocytes were field stimulated, and contractility and Fura-2 fluorescence were monitored with an IonOptix setup configured with 360- and 380-nm excitation filters, a 400-nm dichroic mirror, and a 510 ± 40-nm emission filter. A fluorescence ratio (360 nm/380 nm) was used to assess diastolic and systolic Ca^{2+} and amplitude of the Ca^{2+} transient (Petroff et al., 2000).

Ca^{2+} restitution protocols

Restitution of Ca^{2+} transients was explored by applying an extra stimulation pulse (S_2) with respect to the regular pacing pulses

Downloaded from http://rupress.org/jgp/article-pdf/152/11/e201912512/1801170/jgp_201912512.pdf by guest on 10 February 2026

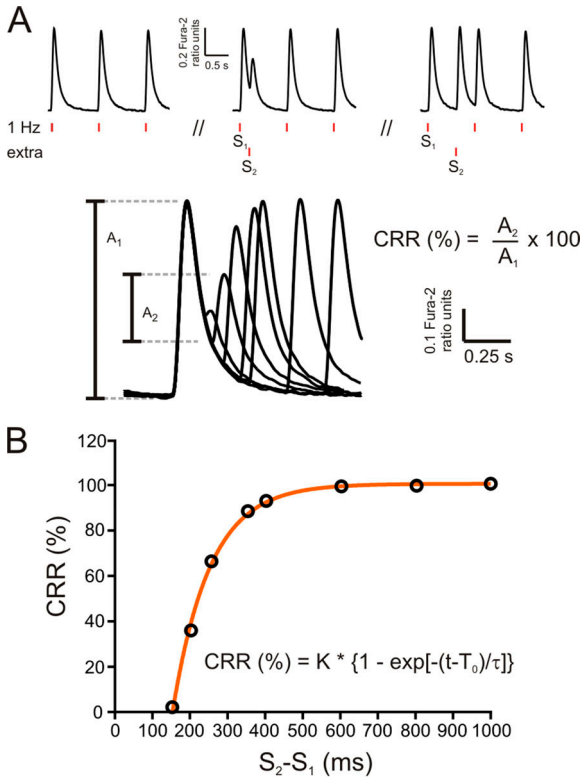

Figure 1. **Experimental protocol. (A)** Experimental protocol used to assess cytosolic Ca^{2+} release refractoriness in mouse myocytes using electrical field stimulation. Vertical red dashes below the typical records (S_1 and S_2) denote basal stimulation frequency (1 Hz) and the extra stimulus, respectively. After a brief conditioning period at 1 Hz, the extra stimulus S_2 was applied at successively shorter S_2-S_1 coupling intervals. Bottom: A typical experimental curve. A_1, amplitude of the Ca^{2+} transient during regular pacing; A_2, amplitude of the Ca^{2+} transient after the extra systolic stimulation. CRR was calculated as the percentage ratio between A_2 and A_1. **(B)** CRR plotted as a function of S_2-S_1 interval. Points could be well fitted by an exponential function. The time constant of this function (τ) was used to estimate the rate of CRR.

(S_1) at different time intervals (S_2-S_1 coupling intervals), as shown in Fig. 1 A. At each time interval, cytosolic Ca^{2+} transient recovery was calculated as the percentage S_2 (A_2) and S_1 (A_1) ratio amplitudes, using the following equation:

$$CRR\ (\%) = \frac{A_2}{A_1} \times 100.$$

CRR (%) was plotted as a function of the (S_2-S_1) coupling interval (Fig. 1 B) to obtain CRR curves. CRR curves were well fitted by a single exponential function, and the time constant of the exponential growth (τ) was obtained.

SR Ca^{2+} content was assessed by rapid application of a 10 mM caffeine pulse. Pulses were applied in the absence of field electrical stimulation.

Measurements of Ca^{2+} currents

The ICaL was recorded with whole-cell configuration of the patch-clamp technique using voltage-clamp configuration. An Axopatch 200B amplifier (Molecular Devices) and a Digidata 1200 analog-to-digital converter (Axon Instruments) were used to acquire ICaL with pClamp 6 software (Molecular Devices). The voltage protocol was performed with a sampling rate of 5 kHz and a low pass filter of 2 kHz. To record the I-V relationship, currents were evoked from a holding potential of −80 mV to a 200-ms prepulse of −40 mV and subsequently to 500-ms test pulses ranging from −40 mV to +35 mV, in 5-mV increments, with a stimulus frequency of 0.1 Hz. Nifedipine (50 µM) completely blocked the currents evoked by the I-V and restitution protocols (data not shown). The restitution protocol was performed recording the currents evoked from a holding potential of −50 mV (used to inactivate sodium channels) to a 50-ms test pulse of 0 mV (S_1), back to −50 mV, and test pulsed again to 0 mV, with increasing time intervals of 50 ms (S_2). A restitution protocol from a holding potential of −60 mV was also assessed in some experiments. Borosilicate patch pipettes were pulled with a P-97 puller (Sutter Instruments) to a final resistance of 2.5 MΩ. The pipette was filled with (in mM): 135 CsCl, 1 $MgCl_2$, 4 Na_2ATP, 1 EGTA, 10 HEPES, pH 7.4, with CsOH (final concentration of Cs^+, 140 mM). The external solution contained (in mM): 5 CsCl, 120 NaCl, 1 $MgCl_2$, 10 HEPES, 10 triethylammonium chloride, 5 4-aminopyridine, 2 or 4 $CaCl_2$, 5 glucose, pH 7.2, with HCl. The patch-clamp data were processed with ClampFit 10.3 (Molecular Devices) and analyzed using Prism 6 software (GraphPad Software). All experiments were performed at room temperature (22–24°C).

Modeling

A previously employed human myocyte model, the Negroni-Lascano model, based on a modified ten Tusscher–Panfilov structure (ten Tusscher et al., 2004), was used (Mazzocchi et al., 2016). A detailed description of the model is provided in Fig. S1 and the supplemental text (see bottom of PDF).

To simulate the behavior of S2814D and PLN ablated myocytes, an increase in RYR2 Ca^{2+} release or in SERCA2a Ca^{2+} uptake, respectively, was added as appropriate ($S2814D_{sim}$, $PLNKO_{sim}$). These changes were represented as an increase in Ca^{2+} sensitivity of RYR2 (Shannon et al., 2005) to obtain an increase in the open probability (conductance) of RYR2 similar to that described experimentally by van Oort et al. (2010), working in S2814D myocytes, and as a decrease in SERCA2a K_d, to obtain an increase in SERCA2a activity similar to that described in PLNKO (Luo et al., 1994), respectively. Moreover, to compare the model with the experimental data, $PLNKO_{sim}$ myocytes were complemented with a 33% decrease in RYR2 conductance to reproduce the reported compensatory decrease in RYR2 expression of PLNKO mouse myocytes (Chu et al., 1998; Mazzocchi et al., 2016). These simulated conditions allowed us to study the effect of RYR2 activity and SR Ca^{2+} reuptake on CRR as a function of SR Ca^{2+}. $SDKO_{sim}$ was simulated as the combination of the $S2814D_{sim}$ and $PLNKO_{sim}$ alterations. We have already shown that the model mimicked the behavior of mouse myocytes in the different strains (Mazzocchi et al., 2016).

After 100 beats of stabilization at a frequency of 70 stimuli/min, an extra stimulus was applied at different, increasingly shorter times from the onset of the last stabilized stimulated beat (beat number 100). Restitution of SR Ca^{2+} release through RYR2 (Irel) in micromoles of Ca^{2+} per millisecond, Ca^{2+} transient (CRR) in micromoles of $[Ca^{2+}]_i$, and ICaL in picoamperes were

Downloaded from http://rupress.org/jgp/article-pdf/152/11/e201912512/1801170/jgp_201912512.pdf by guest on 10 February 2026

measured in the human myocyte model that mimics WT, S2814D, PLNKO, and SDKO mouse conditions at external Ca^{2+} concentrations yielding stabilized beats free from arrhythmias (1.5–2.5 mM). Ca^{2+} restitution curves were fitted to an exponential function, and the exponential time constant, τ, was plotted as a function of SR Ca^{2+} load at each extracellular Ca^{2+} concentration. Of note, in the mathematical model, it is possible to evaluate either the restitution of Ca^{2+} transients (CRR) or to directly compute the restitution of Irel, thus avoiding post-release mechanisms that can influence the shape of the Ca^{2+} transient. As shown in Fig. S2, Ca^{2+} transients or Irel restitution curves have similar behavior in the human myocyte model. Therefore, we used Irel to estimate CRR in the mathematical model, unless otherwise stated.

Statistics

Continuous variables were expressed as mean ± SEM. When several cells per animal were used, results of the number of cells in each animal were averaged. The number used for statistical analysis corresponds to the number of animals. Results were compared with either unpaired Student's *t* test or one-way ANOVA followed by Tukey's post hoc test, as appropriate. $P < 0.05$ was considered significant. Graph Pad Prism 6.0 software package was used for statistical analyses.

Online supplemental material

Fig. S1 shows a schematic diagram of the model. Fig. S2 demonstrates that Ca^{2+} transients or Irel restitution curves have a similar behavior in the human myocyte model. Fig. S3 shows that pseudophosphorylation of RYR2 at the Ser2814 site (S2814D) significantly increases maximal density of high-affinity [^{3}H]ryanodine binding sites and the frequency of SR Ca^{2+} sparks. Fig. S4 displays raw data of the experimental protocol used to determine CRR curves. Fig. S5 depicts raw data and overall results of ICaL restitution in WT, PLNKO, and S2814D myocytes, recorded at 0 mV from a holding potential of −60 mV. Fig. S6 shows that the increase in extracellular Ca^{2+} and the ablation of PLN enhance ICaL inactivation kinetics. Fig. S7 shows Western blots and overall results of the decreased expression of RYR2 in PLNKO and SDKO mouse hearts and indicates that Casq2 expression does not significantly change in S2814D, PLNKO, and SDKO with respect to WT mouse hearts.

Results

Restitution of SR Ca^{2+} release is enhanced by increasing SR Ca^{2+} load

To explore the effects of increasing SR Ca^{2+} content on CRR, we created CRR curves in myocytes from WT mice at two different extracellular Ca^{2+} concentrations. SR Ca^{2+} content was estimated by caffeine pulses at the same extracellular Ca^{2+} concentrations. Fig. 2 shows that an increase in extracellular Ca^{2+} increases SR Ca^{2+} content both experimentally (Fig. 2 A) and in model simulations (Fig. 2 B). Fig. 2 C depicts typical experimental CRR curves obtained in WT myocytes at 2.0 and 4.0 mM extracellular Ca^{2+}, showing that τ decreases with increasing SR Ca^{2+} load (Fig. 2 C, inset). Fig. 2 D shows that similar results were obtained for Irel in the human myocyte model; that is, the increase in SR Ca^{2+} enhanced Irel restitution (Fig. 2 D, inset). Of note, increasing extracellular Ca^{2+} from 2.0 to 4.0 mM did not affect diastolic $[Ca^{2+}]_i$ significantly (2.0 mM, 1.25 ± 0.03 F/F_0; 4.0 mM, 1.31 ± 0.06 F/F_0; $n = 8$). Taken together, these results indicate that the increase in SR Ca^{2+} load by increasing extracellular Ca^{2+} enhances CRR, as evidenced by the decrease in τ.

CRR was accelerated by PLN ablation and constitutive pseudophosphorylation of RYR2 by CaMKII

It is well known that PLN ablation increases SR Ca^{2+} load by increasing the speed of Ca^{2+} sequestration (Luo et al., 1994). Moreover, it has also been described that pseudophosphorylation of RYR2 at the Ser2814 site increases the activity of RYR2 (Wehrens et al., 2004; Voigt et al., 2012; Mazzocchi et al., 2016; Valverde et al., 2019). This contention is further supported by the results obtained from [^{3}H]ryanodine binding studies in ventricular homogenates and from SR Ca^{2+} sparks in isolated myocytes using confocal microscopy (Fig. S3). Pseudophosphorylation of RYR2 at the Ser2814 site (S2814D) significantly increases the maximal density of high-affinity [^{3}H]ryanodine binding sites (Fig. S3 A). In addition, the frequency of SR Ca^{2+} sparks is higher in S2814D than in WT myocytes at 6.0 mM extracellular Ca^{2+} (Fig. S3 B). Normalization of these data by the SR Ca^{2+} content further increases the difference in spark frequency (Fig. S3 B). Confirming previous findings (Wehrens et al., 2004; van Oort et al., 2010; Mazzocchi et al., 2016; Valverde et al., 2019), these results indicate that CaMKII-dependent phosphorylation of RYR2 enhances the activity of the channels.

Previous experiments have shown that increasing SR Ca^{2+} refilling (PLNKO) accelerates CRR (Szentesi et al., 2004). Moreover, increasing RYR2 activity decreases its refractoriness (Wang et al., 2014; Sun et al., 2018) and enhances CRR (Sun et al., 2018). We evaluated the hypothesis that CRR is accelerated by the increased activity of RYR2 produced by pseudophosphorylation of RYR2 at the S2814 site in S2814D mice and is further enhanced when both alterations (i.e., increasing SR Ca^{2+} refilling and RYR2 activity) are present, like in SDKO myocytes. Fig. 3 A shows typical raw data of the experimental protocol used. Fig. S4 shows, in more detail, the experimental protocol for all four strains. Fig. 3 B shows CRR curves obtained in WT, S2814D, PLNKO, and SDKO myocytes at the same extracellular Ca^{2+} concentration (2.0 mM). Fig. 3 C shows similar behavior in the human myocyte model mimicking the different genetically altered mice. Fig. 3 D shows overall experimental results of τ values of CRR of the four mouse models, which were reproduced by the human myocyte model in Fig. 3 E. As expected, τ was significantly decreased in PLNKO and SDKO myocytes relative to WT myocytes. In contrast, τ values were similar (only slightly lower) in S2814D versus WT myocytes and did not decrease in SDKO versus PLNKO myocytes, despite the enhanced activity of RYR2 in S2814D and SDKO.

A possible explanation in interpreting these somewhat unexpected results can stand on the fact that CRR also depends on the electrical activity of cardiomyocytes (i.e., the action potential [AP] recovery) and, more important, the associated ICaL, which

Downloaded from http://rupress.org/jgp/article-pdf/152/11/e201912512/1801170/jgp_201912512.pdf by guest on 10 February 2026

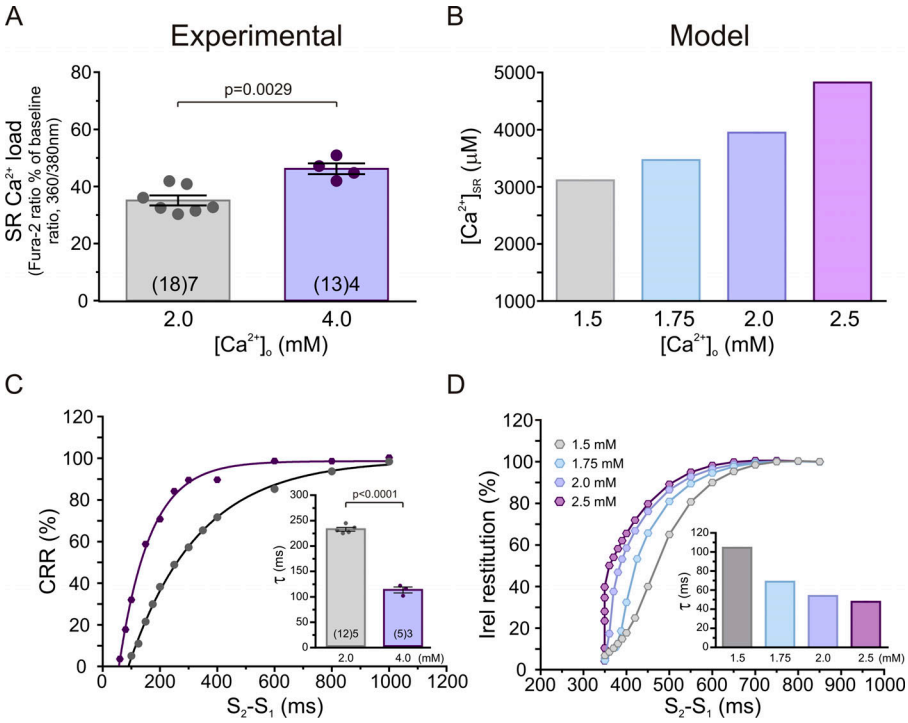

Figure 2. **The increase in SR Ca^{2+} content enhances CRR and Irel. (A)** SR Ca^{2+} content estimated by applying a caffeine pulse of 10 mM in the absence of electrical stimulation. **(B)** SR Ca^{2+} content obtained in the model at different extracellular Ca^{2+} concentrations in WT myocytes. **(C)** Typical CRR curves and overall results of τ values of CRR (inset) at 2.0 and 4.0 mM extracellular Ca^{2+}. **(D)** Irel restitution curves obtained in the model at different extracellular Ca^{2+} concentrations. The increase in extracellular Ca^{2+} from 2.0 to 4.0 mM increased SR Ca^{2+} content and decreased τ in WT myocytes. Similar results were obtained in the human myocyte model mimicking WT myocytes when extracellular Ca^{2+} was increased from 1.5 to 2.5 mM. Experimental data are expressed as mean ± SEM. Numbers inside bars represent the number of animals used; numbers within parentheses inside bars represent the number of cells. When several cells per animal were used, results of the number of cells in each animal were averaged. The numbers used for statistical analysis correspond to the number of animals. P values are denoted above the bars.

determines CICR (Fabiato and Fabiato, 1977). Previous experiments performed in the intact heart showed that the AP restitution did not differ between S2814D and SDKO hearts (Mazzocchi et al., 2016). In preliminary experiments, we further observed that AP restitution in PLNKO and WT was also similar to that previously described in SDKO and S2814D hearts. These results would indicate that AP restitution was not responsible for the CRR differences observed among the different strains. However, all these experiments were performed in the intact heart and at a different temperature and may not reflect the restitution of ICaL. We therefore performed voltage-clamp experiments in isolated myocytes to examine possible changes produced by PLN ablation and RYR2 pseudophosphorylation on ICaL as the trigger for Ca^{2+} release. The effect of increasing extracellular Ca^{2+} was also examined. Fig. 4 A shows that I-V relationships were similar in WT, PLNKO, and S2814D myocytes. As expected, ICaL increased when extracellular Ca^{2+} was increased from 2.0 to 4.0 mM Ca^{2+}. Fig. 4 B depicts original traces of the protocol used to assess ICaL restitution kinetics in the different strains and in WT myocytes at 2.0 and 4.0 mM Ca^{2+}, and Fig. 4, C and E, shows experimental ICaL restitution curves. Increasing extracellular Ca^{2+} from 2.0 to 4.0 mM enhanced ICaL inactivation recovery (Fig. 4 C). Similar results were obtained in the mathematical model when extracellular Ca^{2+} was increased (Fig. 4 D). These findings indicate that the faster recovery of ICaL at 4.0 mM Ca^{2+} may influence the faster recovery of CRR and Irel at the higher extracellular Ca^{2+} concentrations. In contrast, PLN ablation or Ser2814 pseudophosphorylation did not significantly alter ICaL restitution (Fig. 4 E). The mathematical model reproduced the experimental data (Fig. 4 F). Similar results were obtained when a holding potential closer to resting membrane potential was employed (−60 mV) and consequently ICaL restitution was accelerated. As shown in Fig. S5, the recovery from inactivation of ICaL (measured in this case as the nifedipine-sensitive current) was still similar among the different mouse strains studied, further supporting the contention that ICaL restitution cannot account for the enhanced CRR produced by PLN ablation or CaMKII-dependent activation of RYR2. A possible limitation of these ICaL measurements is that the myocytes were dialyzed with EGTA, which may prevent the physiological Ca^{2+}-dependent ICaL inactivation, impacting the extent of recovery from inactivation. The EGTA concentration used in the present experiments (1 mM) causes resting [Ca^{2+}] to be low and can effectively prevent SERCA-dependent SR Ca^{2+} uptake and subsequent SR Ca^{2+} release, a major component of Ca^{2+}-dependent inactivation. However, this concentration of EGTA is well below the one used in experiments in which Ca^{2+}-dependent inactivation of ICaL was explored. Intracellular dialysis with much higher concentrations of this slow Ca^{2+} buffer (5–10 mM) has been reported as poorly effective to buffer Ca^{2+} microdomains, allowing the detection of ICaL Ca^{2+}-dependent inactivation produced by Ca^{2+} entry through the channel and/or Ca^{2+} released through RYR2 (Masaki et al., 1997; Sham, 1997; You et al., 1997). Indeed, studying the inactivation kinetics of the current, we were able to detect faster ICaL inactivation in WT myocytes exposed to high extracellular Ca^{2+} or in PLNKO than in WT or S2814D myocytes exposed to 2.0 mM Ca^{2+} (Fig. S6). These findings reflect a greater ICaL Ca^{2+}-dependent inactivation induced by the enhanced RYR2 release of Ca^{2+} in WT myocytes at 4.0 mM and in PLNKO myocytes.

A second possibility to explain the results of Fig. 3 may be associated with the different SR Ca^{2+} contents that the four mouse models have at the same extracellular Ca^{2+} concentration (2.0 mM) at which τ values were obtained. As shown in Fig. 5 A, SR Ca^{2+} content at 2.0 mM extracellular Ca^{2+} varies significantly in the different mouse models: It was lower in S2814D than in

Downloaded from http://rupress.org/jgp/article-pdf/152/11/e201912512/1801170/jgp_201912512.pdf by guest on 10 February 2026

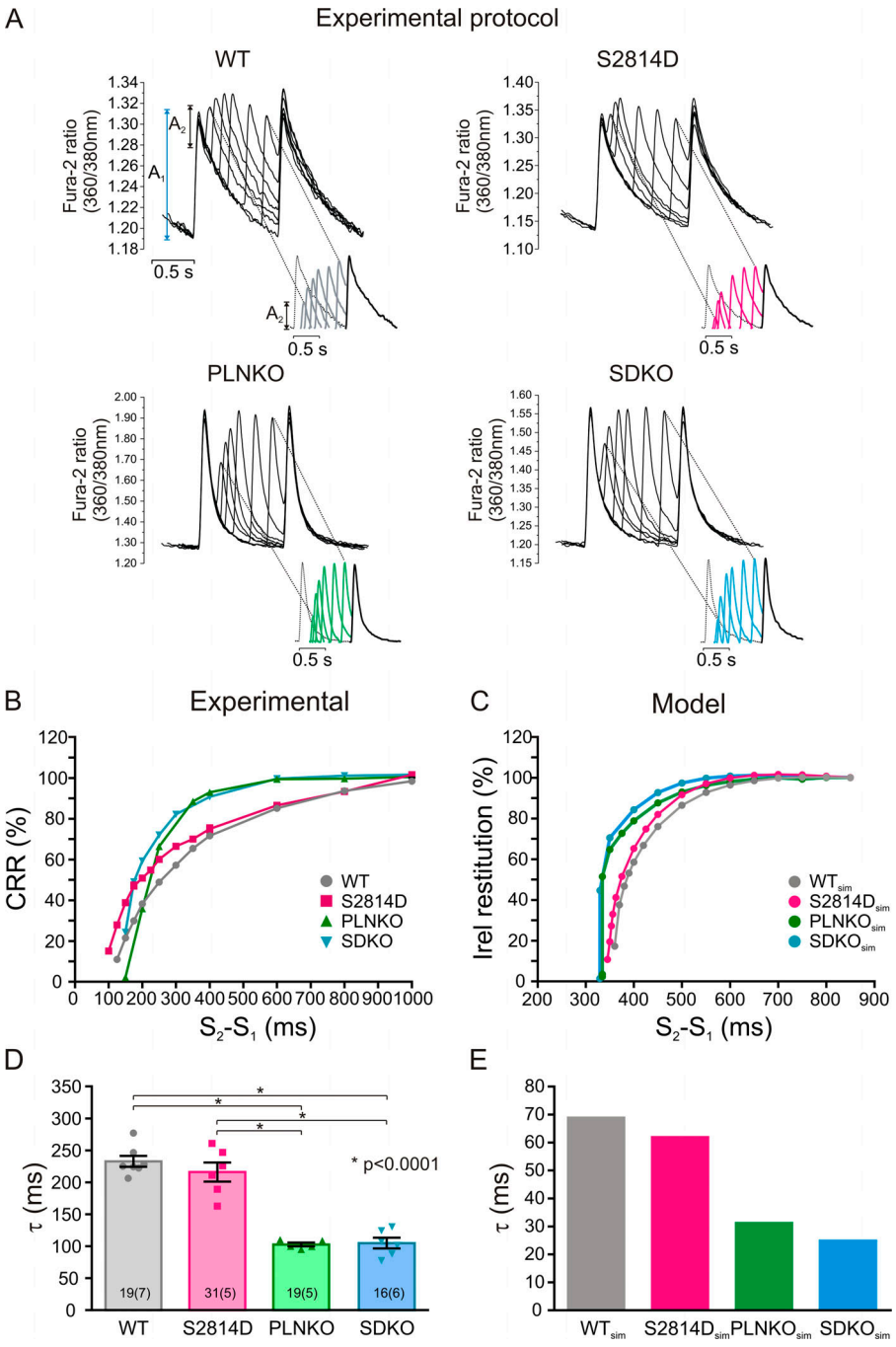

Figure 3. **CRR is different in the different mouse strains. (A)** Typical raw data obtained in WT, S2814D, PLNKO, and SDKO myocytes at 2.0 mM extracellular Ca^{2+}. A_1 and A_2 indicate the amplitude of the Ca^{2+} transient during regular pacing and after the extra systolic stimulation, respectively. The insets below show the progression of A_2 values in the different strains. **(B and C)** Typical experimental CRR curves obtained in the four strains (B) and CRR curves in the human myocyte model mimicking the mouse strains (C) at the same extracellular Ca^{2+} concentration (2.0 mM). **(D)** Overall experimental results of τ values of the four strains. **(E)** τ values obtained in the human model mimicking the four strains. τ was slightly but not significantly reduced in S2814D versus WT myocytes and significantly reduced in PLNKO and SDKO myocytes with respect to both WT and S2814D myocytes. The model reproduced the experimental data. Experimental data are expressed as mean ± SEM. Numbers inside bars represent the number of animals used; numbers within parentheses inside bars represent the number of cells. When several cells per animal were used, results of the number of cells in each animal were averaged. The numbers used for statistical analysis correspond to the number of animals. P values are denoted above the bars.

WT, reaching significant levels when compared by unpaired Student's *t* test, with a P value of 0.0125, and in SDKO versus PLNKO myocytes, as expected by the enhanced RYR2 activity (van Oort et al., 2010; Mazzocchi et al., 2016) and on the basis of the present results (Fig. S7). Moreover, this parameter was significantly higher in PLNKO than in WT and nearly significant in SDKO myocytes versus S2814D myocytes, reaching significant levels when compared by unpaired Student's *t* test (P = 0.0006), as expected by ablation of PLN (Luo et al., 1994). Indeed, and in agreement with previous findings (Mazzocchi et al., 2016), the ablation of PLN (PLNKO and SDKO) significantly decreased τ values of Ca^{2+} transient decay (Fig. 5 C). The myocyte model shows results similar to those for the experimental data in mice (Fig. 5, B and D). Taken together, these findings indicate that the values of τ observed in the different mouse models may be affected by the differences in SR Ca^{2+} contents. For instance, the similar τ values of S2814D versus WT and of SDKO versus PLNKO seen in Fig. 3, despite the lower SR Ca^{2+} content of S2814D and SDKO with respect to WT and PLNKO, respectively (Fig. 5), would suggest that, for the same SR Ca^{2+} content, the increased activity of RYR2 decreases τ. However, the role of RYR2 activity on τ, at a given SR Ca^{2+} content, remains speculative on the basis of these results. Moreover, it was not possible to differentiate between the potential independent role of the speed of Ca^{2+} sequestration and that of SR Ca^{2+} content itself on CRR (i.e., whether the enhancement of CRR observed in PLNKO and SDKO myocytes with respect

Downloaded from http://rupress.org/jgp/article-pdf/152/11/e201912512/1801170/jgp_201912512.pdf by guest on 10 February 2026

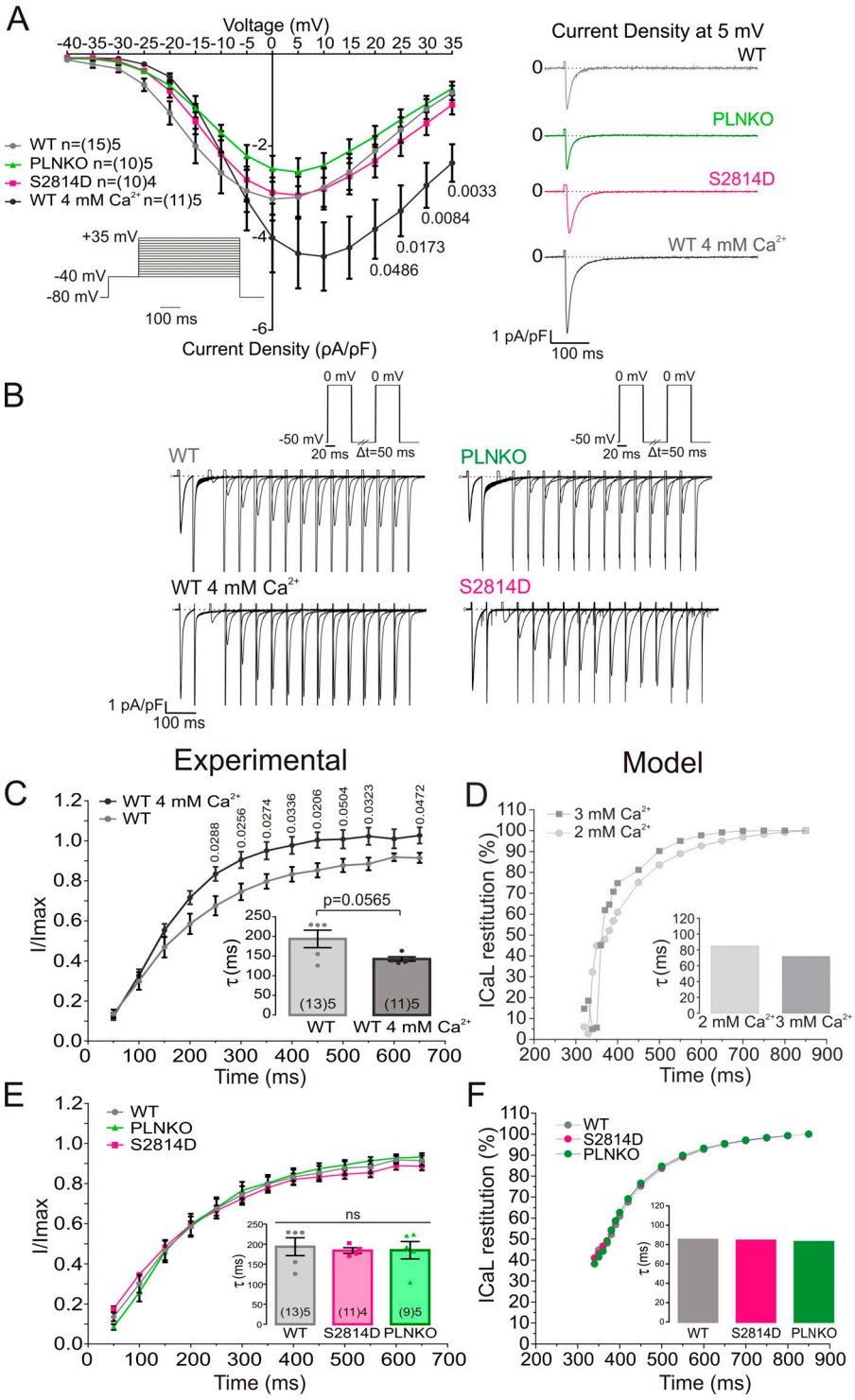

Figure 4. **The different strains have similar ICaL and ICaL restitution. (A)** I-V relationship was similar in WT, PLNKO, and S2814D myocytes and was enhanced with increasing extracellular Ca^{2+}. **(B)** Original traces of the protocol used to assess ICaL restitution kinetics. **(C and D)** Experimental and model results, respectively, of ICaL restitution curves showing that ICaL inactivation recovery is enhanced by increasing extracellular Ca^{2+}. **(E and F)** Experimental and model results, respectively, of ICaL restitution curves. Ablation of PLN or increased RYR2 activity by RYR2 Ser2814 pseudophosphorylation did not significantly alter ICaL restitution. Experimental data were expressed as mean ± SEM. Numbers inside bars represent the number of animals used; numbers within parentheses inside bars represent the number of cells. When several cells per animal were used, results of the number of cells in each animal were averaged. The numbers used for statistical analysis correspond to the number of animals. P values are denoted above the bars.

to WT and S2814D, respectively, may be explained by either the higher SR Ca^{2+} load or the increased rate of Ca^{2+} refilling typical of these two mouse models).

Computational simulation predicts that CRR is determined by SR Ca^{2+} load, Ca^{2+} sensitivity of RYR2, and velocity of SR Ca^{2+} reuptake

In an attempt to unmask the already described effect of RYR2 activity on CRR (Ramay et al., 2011) and to dissect the possible self-reliant role of the two tightly associated variables (i.e., the rate of SR refilling versus SR Ca^{2+} content on CRR), we followed a different strategy. We first interrogated the model by assessing τ values of WT_{sim} and $S2814D_{sim}$ human myocytes at different SR Ca^{2+} concentrations obtained by increasing extracellular Ca^{2+}. With this approach, the influence of the increase in RYR2 activity on τ could be explored at the same SR Ca^{2+} load. The points follow two distinct curves: the $S2814D_{sim}$ curve running approximately parallel to and below the WT_{sim} curve (Fig. 6 A, gray

Downloaded from http://rupress.org/jgp/article-pdf/152/11/e201912512/1801170/jgp_201912512.pdf by guest on 10 February 2026

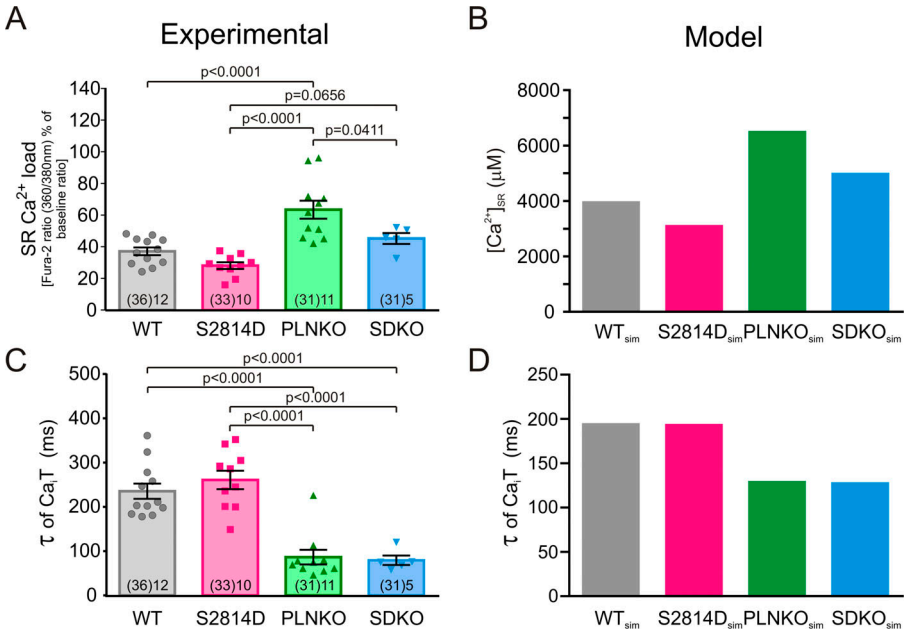

Figure 5. **The different strains have different SR Ca^{2+} loads at 2.0 mM extracellular Ca^{2+}. (A)** SR Ca^{2+} load estimated by rapid caffeine pulses at 2.0 mM extracellular Ca^{2+} in the different mouse strains. **(B)** SR Ca^{2+} loads obtained in the human myocyte model, mimicking WT, S2814D, PLNKO, and SDKO mouse myocytes. **(C and D)** Experimental and model τ values of Ca^{2+} transient decay. Experimental data are expressed as mean ± SEM. Numbers inside bars represent the number of animals used; numbers within parentheses inside bars represent the number of cells. When several cells per animal were used, results of the number of cells in each animal were averaged. The numbers used for statistical analysis correspond to the number of animals. P values are denoted above the bars.

and magenta full circles). These results indicate that CRR is faster in $S2814D_{sim}$ myocytes than in WT_{sim} myocytes for a given SR Ca^{2+} load. We then plotted τ values of $PLNKO_{sim}$ and $SDKO_{sim}$ myocytes and the corresponding SR Ca^{2+} contents obtained at two different extracellular Ca^{2+} concentrations. We hypothesized that if the rate of Ca^{2+} refilling plays a role in CRR different from that of the SR Ca^{2+} load, the $PLNKO_{sim}$ and $SDKO_{sim}$ myocyte data would fall below the WT_{sim} and $S2814D_{sim}$ curves, respectively; that is, for a given SR Ca^{2+} load, τ would be lower. Fig. 6 A indicates that this was not the case. $PLNKO_{sim}$ τ values (green full circles) fell in the WT_{sim} curve, whereas $SDKO_{sim}$ τ points (light blue full circles) could be fitted to the $S2814D_{sim}$ curve. To compare whether the experimental results obtained in mouse myocytes followed a pattern similar to that of the human myocyte model, the obtained experimental and modeling results of τ and SR Ca^{2+} load are represented in Fig. 6 B as the percentage of their respective WT values obtained at 2.0 mM extracellular Ca^{2+}. As shown, the experimental values (crosses representing mean ± SEM), followed a behavior similar to that of the respective values of the model. PLNKO experimental data (green cross) fell close to the WT_{sim} curve, whereas S2814D and SDKO experimental data (magenta and light blue crosses, respectively) fell close to the $S2814D_{sim}$ curve. Although at first sight these results would indicate that the velocity of SR Ca^{2+} reuptake does not play a significant role in the determination of CRR, a limitation of PLN ablated mice (PLNKO and SDKO) is that RYR2 expression has been described to be reduced between 27% (Chu et al., 1998) and 33% (Mazzocchi et al., 2016) with respect to WT mice, as was confirmed in the experimental data shown in Fig. S7 A.

As stated in the Materials and methods, the human myocyte model mimicked this decrease. Decreasing the number of active RYR2 sites led to a decrease in the Ca^{2+} released for a given SR Ca^{2+} load (Zima et al., 2008), which would affect CRR. To avoid the effects of RYR2 underexpression in mice with ablation of PLN, we used the human myocyte model to calculate τ values in $PLNKO_{sim}$ and $SDKO_{sim}$ at different SR Ca^{2+} concentrations without introducing the change in RYR2 typical of these mice. Fig. 6 B shows that the points corresponding to $PLNKO_{sim}$ and $SDKO_{sim}$ without the correction for the decrease in RYR2 expression (i.e., noncompensated $PLNKO_{sim}$ and $SDKO_{sim}$ [$PLNKO_{NC}$, green squares; $SDKO_{NC}$, light blue squares]) fell below the corresponding WT_{sim} and $S2814D_{sim}$ curves. Thus, by correcting in the model the decreased RYR2 expression evoked by PLN ablation, these model curves move to the left. We suggest that this might be an effect of the increase in SR Ca^{2+} reuptake and that the velocity of SR Ca^{2+} refilling might have an effect on CRR that differs from that of SR Ca^{2+} load itself. Although this could be a time-dependent manifestation of [Ca^{2+}] SR, further experimental studies are necessary to validate this intriguing point.

Discussion

The beat-to-beat stability of CICR is essential to maintaining normal cardiac function. Indeed, a large amount of experimental evidence has associated the instability of cytosolic Ca^{2+} transient amplitude with the propensity to cardiac alternans and the risk for ventricular arrhythmias and sudden cardiac arrest (Díaz et al., 2002; Terentyev et al., 2002, 2003; Szentesi et al., 2004; Wang et al., 2014; Kanaporis and Blatter, 2015; Sun et al., 2018). The essential mechanism underlying beat-to-beat stability is CRR. Several previous studies support the notion that SR Ca^{2+} refilling as well as RYR2 activity are main determinants of CRR at the subcellular and cellular levels (Szentesi et al., 2004; Terentyev et al., 2008; Ramay et al., 2011). However, some fundamental questions remain unanswered, including the possible independent influence of the velocity of Ca^{2+} refilling versus SR Ca^{2+} content on the recovery of Ca^{2+} release.

Downloaded from http://rupress.org/jgp/article-pdf/152/11/e201912512/1801170/jgp_201912512.pdf by guest on 10 February 2026

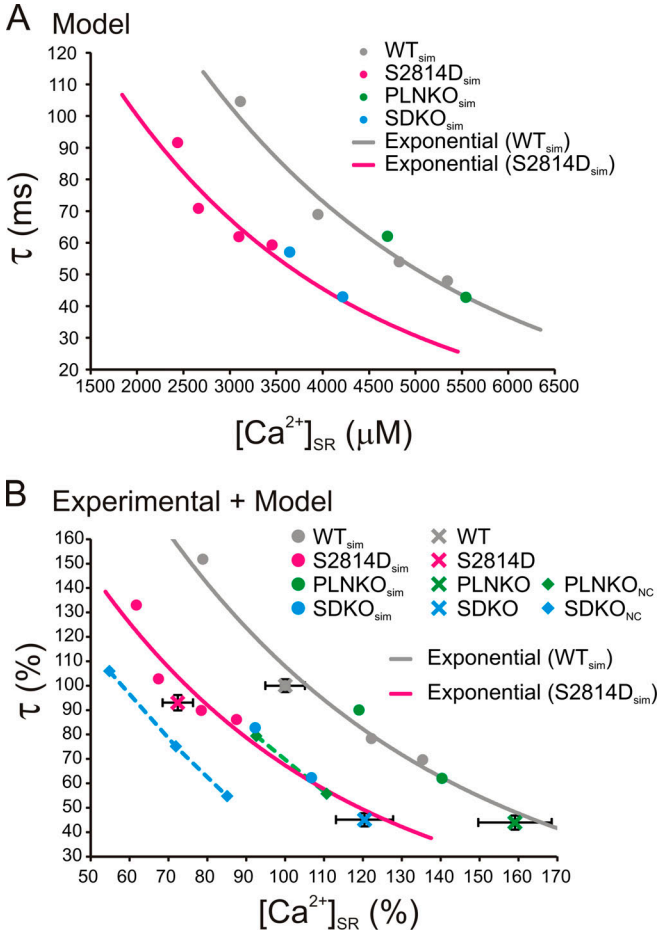

Figure 6. **CRR is enhanced by the increase in SR Ca^{2+} content, the CaMKII-dependent increased activity of RYR2, and the velocity of SR Ca^{2+} reuptake. (A)** Mathematical model curves showing τ as a function of SR Ca^{2+} load in human myocytes mimicking WT (gray) and S2814D (magenta) myocytes. τ decreases with increasing SR Ca^{2+} load in both WT_{sim} and $S2814D_{sim}$ following two different exponential curves which indicate that, for a given SR Ca^{2+} load, τ is lower in $S2814D_{sim}$. The green and light blue full circles indicate the relationship between τ and SR Ca^{2+} load in $PLNKO_{sim}$ and $SDKO_{sim}$ myocytes. The points fell in the WT_{sim} and $S2814D_{sim}$ curves, respectively. **(B)** The same curves of A are represented as percentage τ values and SR Ca^{2+} loads obtained in WT_{sim} myocytes at 2.0 mM extracellular Ca^{2+} to allow comparison with the experimental CRR data, similarly expressed as percentage values. As shown, the experimental points (crosses) of WT and PLNKO myocytes fell in the WT_{sim} curve, whereas the experimental points of S2814D and SDKO myocytes fell in the $S2814D_{sim}$ curve. Green and light blue squares represent τ values at different SR Ca^{2+} loads in $PLNKO_{sim}$ and $SDKO_{sim}$ human myocytes without the compensatory decrease (non-compensated, NC) in the expression of RYR2 produced by PLN ablation ($PLNKO_{NC}$ and $SDKO_{NC}$). As shown, the points follow a curve (dashed line) that is below the respective WT_{sim} and $S2814D_{sim}$ curves, indicating that for the same SR Ca^{2+} load, the increase in the velocity of Ca^{2+} refilling decreases τ (enhances Irel restitution) independently of the effect of SR Ca^{2+} content on CRR. Experimental data are expressed as mean ± SEM.

In the present study, we employed a knock-in mouse model harboring a mutation of RYR2 at the Ser2814 site (S2814D) to enhance the activity of RYR2 (Wehrens et al., 2004; van Oort et al., 2010; Mazzocchi et al., 2016), the PLNKO mouse model, to enhance SR Ca^{2+} reuptake and refilling (Luo et al., 1994), and the SDKO mouse model (Mazzocchi et al., 2016; Valverde et al., 2019). To better define the relative roles of the different players known to determine CRR as well as to dissect the relative importance of the velocity of SR Ca^{2+} refilling versus SR Ca^{2+} load on CRR, we used a previously validated mathematical human myocyte model (Lascano et al., 2013; Mazzocchi et al., 2016). The present results show the following: (1) The increase in SR Ca^{2+} content produced by increasing extracellular Ca^{2+} enhances CRR; (2) the increase in RYR2 activity produced by constitutive pseudophosphorylation of RYR2 at the Ser2814 site increases the velocity of CRR with respect to WT myocytes when compared at the same SR Ca^{2+} content in a wide range of SR Ca^{2+} contents; and (3) the enhanced velocity of SR Ca^{2+} refilling accelerates CRR independently of the associated increase in SR Ca^{2+} load.

CRR is enhanced by increasing SR Ca^{2+} content

To investigate the role of SR Ca^{2+} content in CRR, we increased SR Ca^{2+} content by increasing extracellular Ca^{2+}. We concluded on the basis of these experiments that the increase in SR Ca^{2+} content decreases τ; that is, it enhances CRR. However, the strategy used to increase SR Ca^{2+} load entails the difficulty that the increase in extracellular Ca^{2+} may affect cytosolic Ca^{2+}. Experimental evidence obtained in past decades suggests that Ca^{2+} refractoriness is probably mediated by mechanisms that reside in the luminal side of the SR (Jiang et al., 2004; Sobie and Lederer, 2012). However, RYR2 opening rate may also be influenced by changes in local diastolic Ca^{2+}, either directly or through the activation of calmodulin (CaM), known to inhibit RYR2 and ICaL (Søndergaard et al., 2015; Vassilakopoulou et al., 2015), or by the enhancement of CaMKII activity, known to produce the opposite effects (Yuan and Bers, 1994; van Oort et al., 2010). The present results indicated that diastolic Ca^{2+} did not change significantly when increasing extracellular Ca^{2+}, which makes improbable any influence of cytosolic Ca^{2+} on the enhancement of CRR observed when SR Ca^{2+} was under this condition. However, we are aware of the fact that a moderate increase in diastolic Ca^{2+} might not have been detected by the fluorescence method used to measure intracellular Ca^{2+}. Moreover, and possibly more important, the increase in SR Ca^{2+} release produced by increasing extracellular Ca^{2+} or that observed in PLNKO and SDKO myocytes with respect to WT or the enhanced SR Ca^{2+} leak of S2814D may locally enhance cytosolic Ca^{2+} and, by activating CaM, inhibit RYR2 (Xu and Meissner, 2004) and slow CRR (Sun et al., 2018). If this were the case, our results would have underestimated the increase in CRR velocity produced when extracellular Ca^{2+} was increased or that observed in PLNKO, SDKO, and S2814D with respect to WT myocytes. However, the effect of cytosolic Ca^{2+} on CRR is not completely clear, and possible additional actors may be playing a role. For instance, an increase in diastolic Ca^{2+} may also stimulate CaMKII and phosphorylate RYR2 (Wehrens et al., 2004), which would help to accelerate CRR and would tend to counteract the activation of CaM, except in S2814D and SDKO myocytes, in which the RYR2 CaMKII site cannot be phosphorylated. In these latter cases, the sole influence of CaM activation would again underestimate the increase in the CRR observed. Thus, the present results cannot discard a possible

Downloaded from http://rupress.org/jgp/article-pdf/152/11/e201912512/1801170/jgp_201912512.pdf by guest on 10 February 2026

influence of putative changes in cytosolic Ca^{2+} on the values of CRR observed, although the above reasoning would suggest that this influence, if any, would underestimate the observed acceleration of CRR under the different conditions.

Increasing RYR2 activity by constitutive pseudophosphorylation of RYR2 enhances CRR

Previous experiments have shown that β-adrenoceptor stimulation enhances CRR (Szentesi et al., 2004; Ramay et al., 2011; Poláková et al., 2015). Although Ramay et al. (2011) concluded that β-adrenoceptor stimulation increases CRR by enhancing SR Ca^{2+} reuptake through PLN phosphorylation and increasing RYR2 sensitivity, possibly through PKA or CaMKII phosphorylation, Poláková et al. (2015) further indicated that maximal RYR2 activation by PKA and CaMKII phosphorylation was required to enhance CRR. Our experiments describe, for the first time, that the increase in RYR2 sensitivity evoked by constitutive pseudophosphorylation of RYR2 at the CaMKII site is sufficient to increase CRR at a given SR Ca^{2+} load. The reason for this apparent discrepancy with Poláková's results is not currently clear. A potential explanation is that the level of RYR2 sensitization produced by the independent isoproterenol-induced phosphorylation of each site (Ser2814 or Ser2808) may be lower than that evoked by constitutive pseudophosphorylation of Ser2814 (S2814D mice) and therefore not sufficiently high to accelerate CRR.

Increasing the velocity of SR Ca^{2+} refilling enhances CRR

Szentesi et al. (2004) were the first to describe that increasing SR Ca^{2+} refilling enhances CRR. The idea of SR Ca^{2+} refilling encompasses the concept of velocity. Indeed, the authors used PLNKO mice to support their pharmacological findings obtained when the variation of SR Ca^{2+} refilling was produced by the combined use of β-adrenoceptor stimulation and drugs that decrease SERCA2a activity (e.g., thapsigargin). However, these experiments failed to differentiate the effect on CRR of SR Ca^{2+} content, necessarily increased by increasing SR Ca^{2+} sequestration, and the velocity of SR Ca^{2+} refilling. Moreover, the decrease in RYR2 expression presented by PLNKO mice (Chu et al., 1998; Mazzocchi et al., 2016) also precludes a precise analysis of the velocity of SR Ca^{2+} reuptake on CRR. Indeed, the results obtained with the human myocyte model that mimicked PLNKO myocytes indicated that the velocity of SR Ca^{2+} refilling did not influence CRR: The τ value obtained for the $PLNKO_{sim}$ myocyte was similar to that of WT over the same corresponding SR Ca^{2+} loads. To avoid these complications and to dissect the possible independent effects of SR Ca^{2+} content and the velocity of SR Ca^{2+} refilling on CRR, we used a mathematical model able to represent the behavior of a "pure" PLNKO myocyte without compensatory mechanisms on RYR2 ($PLNKO_{NC}$). For this purpose, the activity of SERCA2a was increased by 50%, whereas the expression of RYR2 was left at the normal (WT) level. Similarly, for $PLNKO_{NC}$, the "pure" SDKO myocyte model was built without the correction of RYR2 due to PLN ablation while preserving the increased RYR2 activity of S2814D ($SDKO_{NC}$). The results clearly indicated that the increase in the velocity of refilling increases CRR independently of the action of SR Ca^{2+} content on CRR.

Relative importance of different factors that influence CRR

Previous results using direct $[Ca]_{SR}$ measurements showed that even after complete recovery of SR Ca^{2+} content, RYR2 refractoriness was still present (Picht et al., 2006; Belevych et al., 2012). According to these findings, the rate-limiting factor for CRR appears to be the recovery of RYR2 activity. At first sight, the importance of the rate of SR Ca^{2+} refilling on CRR suggested by the present findings seems to be at odds with these previous results (Picht et al., 2006; Belevych et al., 2012). However, it is important to emphasize that our results cannot establish the relative importance of the different determinants of CRR. Our goal was to dissect different variables that are difficult to separate experimentally because of being tightly intertwined and that may play a role in CRR. In this sense, the use of mutant mice in combination with mathematical modeling proved to be useful. Confirming the previous findings, the results demonstrated that RYR2 refractoriness and SR Ca^{2+} content both play a role in CRR. Mathematical modeling further suggests that the velocity of SR Ca^{2+} refilling is also involved. Despite the extensive evidence indicating the importance of luminal Ca^{2+} on RYR2 gating regulation and RYR2 refractoriness, the specific molecular mechanisms of CRR regulation by luminal Ca^{2+} are not completely clarified. RYR2 regulation by intraluminal Ca^{2+} may occur directly (Jiang et al., 2004, 2007) or indirectly through the involvement of different intraluminal SR proteins, such as CASq2, triadin, and junctin, acting in concert (Zhang et al., 1997; Györke et al., 2004; Knollmann et al., 2006; Chopra et al., 2009), or histidine-rich Ca^{2+}-binding protein (Arvanitis et al., 2011). Increasing SR Ca^{2+} refilling rate may therefore act by accelerating the achievement of the necessary luminal Ca^{2+} level to trigger RYR2 opening and/or by increasing the coupling of Ca^{2+} release units inside the SR (Qu et al., 2013). Indeed, an intriguing finding of the experiments by Belevych et al. (2012) is that the lower SR Ca^{2+} load presented by postinfarction myocytes (associated with an increase of the RYR2 activity) was attained before RYR2 recovery from refractoriness. This finding would suggest a partial recovery of RYR2 unable to evoke spontaneous events but responsible for maintaining the low SR Ca^{2+} content exhibited by these myocytes. If this were the case, an increase in the velocity of SR Ca^{2+} refilling would contribute to favor at least this partial restitution. A second possibility would be that the recovery of RYR2 from refractoriness can proceed only after a given level of SR Ca^{2+} content is reached. In this case, the velocity of SR Ca^{2+} recovery may play an important role in CRR. Further experiments are needed to clarify this intriguing point.

In summary, our experiments confirmed that CRR is determined by SR Ca^{2+} load and RYR2 Ca^{2+} sensitivity. We further raise the possibility that the velocity of SR Ca^{2+} refilling may be an important player in controlling CRR, independent of SR Ca^{2+} content.

Limitations of the study

There are a number of caveats to consider in the present results. Previous studies revealed an expansion of SR volume and downregulation of triadin 1 and junctin in myocytes from $Casq2^{-/-}$ mice, in which SR Ca^{2+} release refractoriness was almost completely absent (Kryshtal et al., 2015). These SR changes

Downloaded from http://rupress.org/jgp/article-pdf/152/11/e201912512/1801170/jgp_201912512.pdf by guest on 10 February 2026

were interpreted as a compensatory mechanism for the loss of SR Ca^{2+} buffering by Casq2, the major intra-SR Ca^{2+} buffering protein (Bers, 2001). As far as we understand, and in contrast to what happens with Casq2$^{-/-}$ mice, there are no apparent reasons to expect a change in the buffer capacity and/or the SR volume in the mouse models used in the present experiments. Indeed, previous experiments in PLNKO showed no apparent changes in the junctional and free SR ultrastructure, organization, and distribution in PLNKO myocytes (Chu et al., 1998). We also considered the possibility that a small change in Casq2 expression in our models could have produced a change in SR volume and buffer capacity, because the 50% increase in SR volume in Casq2$^{-/-}$ mice almost fully compensated for the lack of Casq2 buffering (Bers, 2001). Again, previous experiments indicated that Casq2 expression did not change in PLNKO myocytes (Chu et al., 1998) or in right atrial samples from patients with chronic atrial fibrillation that presented an increase in Ser2814 and Ser2808 phosphorylation of RYR2 (Voigt et al., 2012), which may have produced adaptive changes similar to those that occurred in S2814D myocytes. The present results confirmed that Casq2 expression did not change in any of the mouse strains studied (Fig. S7 B). Thus, although we cannot completely rule out the possibility of changes in SR volume or buffer capacity in our experiments that could have affected our conclusions, this possibility seems unlikely.

We are also aware that another limitation of our study is the difficulty in showing experimentally the importance of the velocity of SR Ca^{2+} refilling as a factor determining CRR independently of SR Ca^{2+} load because of the tight association between these two parameters. The fact that the τ of $[Ca^{2+}]_i$ decline is similar to the CRR τ for all cases, in which the former is an indirect $[Ca^{2+}]_{SR}$ refilling level (Figs. 5 and 3, respectively), supports the critical importance of SR Ca^{2+} content for CRR. Unfortunately, the present experiments cannot distinguish the velocity of SR Ca^{2+} refilling at the moment of release from the level of $[Ca^{2+}]_{SR}$ at that time. However, one advantage of using mathematical models is that they give access to variables that are hard to measure experimentally or that are tightly intertwined. In the present study, the mathematical model proved to reproduce all the experimental data. This strength gives us great confidence in the results predicted by the model. Moreover, the fact that the experimental values of τ of PLNKO and SDKO fall on the curve generated by the model for WT and S2814D, in spite of having a 30% decrease in RYR2 expression (Fig. S7 A), is experimentally in line with the contention that the increase in the velocity of refilling is a determinant of CRR. Future voltage-clamp experiments with real-time $[Ca^{2+}]_{SR}$ measurements are needed to experimentally support the independent role of the velocity of SR Ca^{2+} refilling in CRR suggested by the mathematical model.

Another limitation of our results is that the experiments performed to study recovery of ICaL and CRR were not carried out in the same cell. Moreover, the 50-ms square pulse to 0 mV used to measure ICaL is different from the V_m waveform that drives Ca^{2+} current in the paced myocytes. Although comparison of ICaL recovery with CRR in the same cell would have been a better approach, the results clearly showed that the recovery of the ICaL did not change in the different strains. Therefore, it cannot be responsible for the changes in CRR observed. Moreover, the square pulse protocol is a widely validated protocol reported in the literature to determine ICaL restitution (Tseng, 1988; Vornanen and Shepherd, 1997; Guo and Duff, 2006; Kryshtal et al., 2015).

We used the Negroni-Lascano human myocyte model (Mazzocchi et al., 2016), modified to improve the Ca^{2+} handling properties of the ten Tusscher model (ten Tusscher et al., 2004) by including the Shannon-Bers RYR2 four-state model (Shannon et al., 2004). Therefore, an additional limitation of our study is that we did not use a mathematical mouse myocyte model. However, because the model reproduces experimental results obtained not only in mouse myocytes (Mazzocchi et al., 2016, and the present results) but also in rat, sheep, and canine myocyte experiments performed in other laboratories (Trafford et al., 2000; Greensmith et al., 2014), we can still consider it as a valid tool to interpret our results.

Acknowledgments

David A. Eisner served as editor.

The authors are grateful for the excellent technical assistance of Omar Castillo, Drs. Luciana Sapia and Omar Velez-Rueda, and Mónica Rando, Guillermina Mangioni, and Leandro Di Ciani. The expert support of Dr. Carmen Valdivia in the [^{3}H]ryanodine binding experiments is also greatly acknowledged.

This work was supported by National Research Council (Argentina) grants PIP 0350 and PICT 2014-2524 (to A. Mattiazzi), PICT 2015-3210 (to C.A. Valverde), PICT 2015-3009 (to J. Palomeque), PICT 2017-1567 (to E.A. Aiello), and PICT-2018-03524 (to J.I. Felice); the Fondation Leducq Transatlantic Networks of Excellence Program (to E.G. Kranias); and National Institutes of Health grants R01-HL089598, R01-HL091947, R01-HL117641, and R01-HL147108 (to X.H.T. Wehrens).

The authors declare no competing financial interests.

Author contributions: This work was performed in the laboratory of A. Mattiazzi. E.C. Lascano, J.A. Negroni, J.I. Felice, and A. Mattiazzi were involved in the conception and design of the experiments and interpretation of the data. A. Cely-Ortiz, J.I. Felice, C.A. Valverde, M. Federico, and J. Palomeque performed the experiments and were involved in collection, analysis, and interpretation of the data. E.A. Aiello and L.A. Díaz-Zegarra designed, performed, analyzed, and interpreted the patch-clamp experiments. X.H.T. Wehrens and E.G. Kranias provided the knock-in mice and PLNKO mice, respectively, and were involved in critically revising the manuscript. J.A. Negroni and E.C. Lascano built the model, and J.A. Negroni developed the MATLAB code. J.A. Negroni, E.C. Lascano, J.I. Felice, L.A. Díaz-Zegarra, C.A. Valverde, A. Cely-Ortiz, E.A. Aiello, and A. Mattiazzi were involved in drafting the article and/or revising it critically. All authors approved the final version of the manuscript. All persons designated as authors qualify for authorship, and all those who qualify for authorship are listed.

Submitted: 9 October 2019
Revised: 27 July 2020
Accepted: 21 August 2020

Downloaded from http://rupress.org/jgp/article-pdf/152/11/e201912512/1801170/jgp_201912512.pdf by guest on 10 February 2026

References

Arvanitis, D.A., E. Vafiadaki, D. Sanoudou, and E.G. Kranias. 2011. Histidine-rich calcium binding protein: the new regulator of sarcoplasmic reticulum calcium cycling. *J. Mol. Cell. Cardiol.* 50:43–49. https://doi.org/10.1016/j.yjmcc.2010.08.021

Belevych, A.E., D. Terentyev, R. Terentyeva, H.T. Ho, I. Gyorke, I.M. Bonilla, C.A. Carnes, G.E. Billman, and S. Györke. 2012. Shortened Ca^{2+} signaling refractoriness underlies cellular arrhythmogenesis in a postinfarction model of sudden cardiac death. *Circ. Res.* 110:569–577. https://doi.org/10.1161/CIRCRESAHA.111.260455

Bers, D.M. 2001. Excitation-Contraction Coupling and Cardiac Contractile Force. Second edition. Springer Netherlands, Dordrecht, Netherlands. 427 pp. https://doi.org/10.1007/978-94-010-0658-3

Chopra, N., T. Yang, P. Asghari, E.D. Moore, S. Huke, B. Akin, R.A. Cattolica, C.F. Perez, T. Hlaing, B.E. Knollmann-Ritschel, et al. 2009. Ablation of triadin causes loss of cardiac Ca^{2+} release units, impaired excitation-contraction coupling, and cardiac arrhythmias. *Proc. Natl. Acad. Sci. USA.* 106:7636–7641. https://doi.org/10.1073/pnas.0902919106

Chu, G., D.G. Ferguson, I. Edes, E. Kiss, Y. Sato, and E.G. Kranias. 1998. Phospholamban ablation and compensatory responses in the mammalian heart. *Ann. N. Y. Acad. Sci.* 853(1 CARDIAC SARCO):49–62. https://doi.org/10.1111/j.1749-6632.1998.tb08256.x

DelPrincipe, F., M. Egger, and E. Niggli. 1999. Calcium signalling in cardiac muscle: refractoriness revealed by coherent activation. *Nat. Cell Biol.* 1:323–329. https://doi.org/10.1038/14013

Díaz, M.E., D.A. Eisner, and S.C. O'Neill. 2002. Depressed ryanodine receptor activity increases variability and duration of the systolic Ca^{2+} transient in rat ventricular myocytes. *Circ. Res.* 91:585–593. https://doi.org/10.1161/01.RES.0000035527.53514.C2

Fabiato, A., and F. Fabiato. 1977. Calcium release from the sarcoplasmic reticulum. *Circ. Res.* 40:119–129. https://doi.org/10.1161/01.RES.40.2.119

Faggioni, M., and B.C. Knollmann. 2012. Calsequestrin 2 and arrhythmias. *Am. J. Physiol. Heart Circ. Physiol.* 302:H1250–H1260. https://doi.org/10.1152/ajpheart.00779.2011

Greensmith, D.J., G.L. Galli, A.W. Trafford, and D.A. Eisner. 2014. Direct measurements of SR free Ca reveal the mechanism underlying the transient effects of RyR potentiation under physiological conditions. *Cardiovasc. Res.* 103:554–563. https://doi.org/10.1093/cvr/cvu158

Guo, J., and H.J. Duff. 2006. Calmodulin kinase II accelerates L-type Ca^{2+} current recovery from inactivation and compensates for the direct inhibitory effect of $[Ca^{2+}]_i$ in rat ventricular myocytes. *J. Physiol.* 574:509–518. https://doi.org/10.1113/jphysiol.2006.109199

Györke, I., N. Hester, L.R. Jones, and S. Györke. 2004. The role of calsequestrin, triadin, and junctin in conferring cardiac ryanodine receptor responsiveness to luminal calcium. *Biophys. J.* 86:2121–2128. https://doi.org/10.1016/S0006-3495(04)74271-X

Helms, A.S., F.J. Alvarado, J. Yob, V.T. Tang, F. Pagani, M.W. Russell, H.H. Valdivia, and S.M. Day. 2016. Genotype-Dependent and -Independent Calcium Signaling Dysregulation in Human Hypertrophic Cardiomyopathy. *Circulation.* 134:1738–1748. https://doi.org/10.1161/CIRCULATIONAHA.115.020086

Hüser, J., Y.G. Wang, K.A. Sheehan, F. Cifuentes, S.L. Lipsius, and L.A. Blatter. 2000. Functional coupling between glycolysis and excitation-contraction coupling underlies alternans in cat heart cells. *J. Physiol.* 524:795–806. https://doi.org/10.1111/j.1469-7793.2000.00795.x

Jiang, D., B. Xiao, D. Yang, R. Wang, P. Choi, L. Zhang, H. Cheng, and S.R. Chen. 2004. RyR2 mutations linked to ventricular tachycardia and sudden death reduce the threshold for store-overload-induced Ca^{2+} release (SOICR). *Proc. Natl. Acad. Sci. USA.* 101:13062–13067. https://doi.org/10.1073/pnas.0402388101

Jiang, D., W. Chen, R. Wang, L. Zhang, and S.R. Chen. 2007. Loss of luminal Ca^{2+} activation in the cardiac ryanodine receptor is associated with ventricular fibrillation and sudden death. *Proc. Natl. Acad. Sci. USA.* 104:18309–18314. https://doi.org/10.1073/pnas.0706573104

Kanaporis, G., and L.A. Blatter. 2015. The mechanisms of calcium cycling and action potential dynamics in cardiac alternans. *Circ. Res.* 116:846–856. https://doi.org/10.1161/CIRCRESAHA.116.305404

Knollmann, B.C., N. Chopra, T. Hlaing, B. Akin, T. Yang, K. Ettensohn, B.E. Knollmann, K.D. Horton, N.J. Weissman, I. Holinstat, et al. 2006. Casq2 deletion causes sarcoplasmic reticulum volume increase, premature Ca^{2+} release, and catecholaminergic polymorphic ventricular tachycardia. *J. Clin. Invest.* 116:2510–2520.

Kornyeyev, D., A.D. Petrosky, B. Zepeda, M. Ferreiro, B. Knollmann, and A.L. Escobar. 2012. Calsequestrin 2 deletion shortens the refractoriness of Ca^{2+} release and reduces rate-dependent Ca^{2+}-alternans in intact mouse hearts. *J. Mol. Cell. Cardiol.* 52:21–31. https://doi.org/10.1016/j.yjmcc.2011.09.020

Kryshtal, D.O., O. Gryshchenko, N. Gomez-Hurtado, and B.C. Knollmann. 2015. Impaired calcium-calmodulin-dependent inactivation of Cav1.2 contributes to loss of sarcoplasmic reticulum calcium release refractoriness in mice lacking calsequestrin 2. *J. Mol. Cell. Cardiol.* 82:75–83. https://doi.org/10.1016/j.yjmcc.2015.02.027

Lascano, E.C., M. Said, L. Vittone, A. Mattiazzi, C. Mundiña-Weilenmann, and J.A. Negroni. 2013. Role of CaMKII in post acidosis arrhythmias: a simulation study using a human myocyte model. *J. Mol. Cell. Cardiol.* 60:172–183. https://doi.org/10.1016/j.yjmcc.2013.04.018

Luo, W., I.L. Grupp, J. Harrer, S. Ponniah, G. Grupp, J.J. Duffy, T. Doetschman, and E.G. Kranias. 1994. Targeted ablation of the phospholamban gene is associated with markedly enhanced myocardial contractility and loss of beta-agonist stimulation. *Circ. Res.* 75:401–409. https://doi.org/10.1161/01.RES.75.3.401

Marty, I. 2015. Triadin regulation of the ryanodine receptor complex. *J. Physiol.* 593:3261–3266. https://doi.org/10.1113/jphysiol.2014.281147

Masaki, H., Y. Sato, W. Luo, E.G. Kranias, and A. Yatani. 1997. Phospholamban deficiency alters inactivation kinetics of L-type Ca^{2+} channels in mouse ventricular myocytes. *Am. J. Physiol.* 272:H606–H612.

Mazzocchi, G., L. Sommese, J. Palomeque, J.I. Felice, M.N. Di Carlo, D. Fainstein, P. Gonzalez, P. Contreras, D. Skapura, M.D. McCauley, et al. 2016. Phospholamban ablation rescues the enhanced propensity to arrhythmias of mice with CaMKII-constitutive phosphorylation of RyR2 at site S2814. *J. Physiol.* 594:3005–3030. https://doi.org/10.1113/JP271622

Mundiña-Weilenmann, C., L. Vittone, M. Ortale, G.C. de Cingolani, and A. Mattiazzi. 1996. Immunodetection of phosphorylation sites gives new insights into the mechanisms underlying phospholamban phosphorylation in the intact heart. *J. Biol. Chem.* 271:33561–33567. https://doi.org/10.1074/jbc.271.52.33561

Negroni, J.A., S. Morotti, E.C. Lascano, A.V. Gomes, E. Grandi, J.L. Puglisi, and D.M. Bers. 2015. β-adrenergic effects on cardiac myofilaments and contraction in an integrated rabbit ventricular myocyte model. *J. Mol. Cell. Cardiol.* 81:162–175. https://doi.org/10.1016/j.yjmcc.2015.02.014

Palomeque, J., O.V. Rueda, L. Sapia, C.A. Valverde, M. Salas, M.V. Petroff, and A. Mattiazzi. 2009. Angiotensin II-induced oxidative stress resets the Ca2+ dependence of Ca2+-calmodulin protein kinase II and promotes a death pathway conserved across different species. *Circ. Res.* 105:1204–1212. https://doi.org/10.1161/CIRCRESAHA.109.204172

Peng, W., H. Shen, J. Wu, W. Guo, X. Pan, R. Wang, S.R. Chen, and N. Yan. 2016. Structural basis for the gating mechanism of the type 2 ryanodine receptor RyR2. *Science.* 354. aah5324. https://doi.org/10.1126/science.aah5324

Petroff, M.G., E.A. Aiello, J. Palomeque, M.A. Salas, and A. Mattiazzi. 2000. Subcellular mechanisms of the positive inotropic effect of angiotensin II in cat myocardium. *J. Physiol.* 529:189–203. https://doi.org/10.1111/j.1469-7793.2000.00189.x

Picht, E., J. DeSantiago, L.A. Blatter, and D.M. Bers. 2006. Cardiac alternans do not rely on diastolic sarcoplasmic reticulum calcium content fluctuations. *Circ. Res.* 99:740–748. https://doi.org/10.1161/01.RES.0000244002.88813.91

Poláková, E., A. Illaste, E. Niggli, and E.A. Sobie. 2015. Maximal acceleration of Ca^{2+} release refractoriness by β-adrenergic stimulation requires dual activation of kinases PKA and CaMKII in mouse ventricular myocytes. *J. Physiol.* 593:1495–1507. https://doi.org/10.1113/jphysiol.2014.278051

Pritchard, T.J., and E.G. Kranias. 2009. Junctin and the histidine-rich Ca^{2+} binding protein: potential roles in heart failure and arrhythmogenesis. *J. Physiol.* 587:3125–3133. https://doi.org/10.1113/jphysiol.2009.172171

Qu, Z., M. Nivala, and J.N. Weiss. 2013. Calcium alternans in cardiac myocytes: order from disorder. *J. Mol. Cell. Cardiol.* 58:100–109. https://doi.org/10.1016/j.yjmcc.2012.10.007

Ramay, H.R., O.Z. Liu, and E.A. Sobie. 2011. Recovery of cardiac calcium release is controlled by sarcoplasmic reticulum refilling and ryanodine receptor sensitivity. *Cardiovasc. Res.* 91:598–605. https://doi.org/10.1093/cvr/cvr143

Sham, J.S. 1997. Ca^{2+} release-induced inactivation of Ca^{2+} current in rat ventricular myocytes: evidence for local Ca^{2+} signalling. *J. Physiol.* 500:285–295. https://doi.org/10.1113/jphysiol.1997.sp022020

Shannon, T.R., F. Wang, J. Puglisi, C. Weber, and D.M. Bers. 2004. A mathematical treatment of integrated Ca dynamics within the ventricular myocyte. *Biophys. J.* 87:3351–3371. https://doi.org/10.1529/biophysj.104.047449

Shannon, T.R., F. Wang, and D.M. Bers. 2005. Regulation of cardiac sarcoplasmic reticulum Ca release by luminal [Ca] and altered gating

Downloaded from http://rupress.org/jgp/article-pdf/152/11/e201912512/1801170/jgp_201912512.pdf by guest on 10 February 2026

assessed with a mathematical model. *Biophys. J.* 89:4096–4110. https://doi.org/10.1529/biophysj.105.068734

Shkryl, V.M., J.T. Maxwell, T.L. Domeier, and L.A. Blatter. 2012. Refractoriness of sarcoplasmic reticulum Ca^{2+} release determines Ca^{2+} alternans in atrial myocytes. *Am. J. Physiol. Heart Circ. Physiol.* 302:H2310–H2320. https://doi.org/10.1152/ajpheart.00079.2012

Sobie, E.A., and W.J. Lederer. 2012. Dynamic local changes in sarcoplasmic reticulum calcium: physiological and pathophysiological roles. *J. Mol. Cell. Cardiol.* 52:304–311. https://doi.org/10.1016/j.yjmcc.2011.06.024

Sobie, E.A., L.S. Song, and W.J. Lederer. 2005. Local recovery of Ca^{2+} release in rat ventricular myocytes. *J. Physiol.* 565:441–447. https://doi.org/10.1113/jphysiol.2005.086496

Søndergaard, M.T., X. Tian, Y. Liu, R. Wang, W.J. Chazin, S.R. Chen, and M.T. Overgaard. 2015. Arrhythmogenic calmodulin mutations affect the activation and termination of cardiac ryanodine receptor-mediated Ca^{2+} release. *J. Biol. Chem.* 290:26151–26162. https://doi.org/10.1074/jbc.M115.676627

Sun, B., J. Wei, X. Zhong, W. Guo, J. Yao, R. Wang, A. Vallmitjana, R. Benitez, L. Hove-Madsen, and S.R.W. Chen. 2018. The cardiac ryanodine receptor, but not sarcoplasmic reticulum Ca^{2+}-ATPase, is a major determinant of Ca^{2+} alternans in intact mouse hearts. *J. Biol. Chem.* 293:13650–13661. https://doi.org/10.1074/jbc.RA118.003760

Szentesi, P., C. Pignier, M. Egger, E.G. Kranias, and E. Niggli. 2004. Sarcoplasmic reticulum Ca^{2+} refilling controls recovery from Ca^{2+}-induced Ca^{2+} release refractoriness in heart muscle. *Circ. Res.* 95:807–813. https://doi.org/10.1161/01.RES.0000146029.80463.7d

ten Tusscher, K.H., D. Noble, P.J. Noble, and A.V. Panfilov. 2004. A model for human ventricular tissue. *Am. J. Physiol. Heart Circ. Physiol.* 286:H1573–H1589. https://doi.org/10.1152/ajpheart.00794.2003

ten Tusscher, K.H., and A.V. Panfilov. 2006. Alternans and spiral breakup in a human ventricular tissue model. *Am. J. Physiol. Heart Circ. Physiol.* 291:H1088–H1100. https://doi.org/10.1152/ajpheart.00109.2006

Terentyev, D., S. Viatchenko-Karpinski, H.H. Valdivia, A.L. Escobar, and S. Györke. 2002. Luminal Ca^{2+} controls termination and refractory behavior of Ca^{2+}-induced Ca^{2+} release in cardiac myocytes. *Circ. Res.* 91:414–420. https://doi.org/10.1161/01.RES.0000032490.04207.BD

Terentyev, D., S. Viatchenko-Karpinski, I. Györke, P. Volpe, S.C. Williams, and S. Györke. 2003. Calsequestrin determines the functional size and stability of cardiac intracellular calcium stores: Mechanism for hereditary arrhythmia. *Proc. Natl. Acad. Sci. USA.* 100:11759–11764. https://doi.org/10.1073/pnas.1932318100

Terentyev, D., Z. Kubalova, G. Valle, A. Nori, S. Vedamoorthyrao, R. Terentyeva, S. Viatchenko-Karpinski, D.M. Bers, S.C. Williams, P. Volpe, et al. 2008. Modulation of SR Ca release by luminal Ca and calsequestrin in cardiac myocytes: effects of CASQ2 mutations linked to sudden cardiac death. *Biophys. J.* 95:2037–2048. https://doi.org/10.1529/biophysj.107.128249

Trafford, A.W., M.E. Díaz, G.C. Sibbring, and D.A. Eisner. 2000. Modulation of CICR has no maintained effect on systolic Ca^{2+}: simultaneous measurements of sarcoplasmic reticulum and sarcolemmal Ca^{2+} fluxes in rat ventricular myocytes. *J. Physiol.* 522:259–270. https://doi.org/10.1111/j.1469-7793.2000.t01-2-00259.x

Tseng, G.N. 1988. Calcium current restitution in mammalian ventricular myocytes is modulated by intracellular calcium. *Circ. Res.* 63:468–482. https://doi.org/10.1161/01.RES.63.2.468

Valverde, C.A., G. Mazzocchi, M.N. Di Carlo, A. Ciocci Pardo, N. Salas, M.I. Ragone, J.I. Felice, A. Cely-Ortiz, A.E. Consolini, E. Portiansky, et al. 2019. Ablation of phospholamban rescues reperfusion arrhythmias but exacerbates myocardium infarction in hearts with Ca^{2+}/calmodulin kinase II constitutive phosphorylation of ryanodine receptors. *Cardiovasc. Res.* 115:556–569. https://doi.org/10.1093/cvr/cvy213

van Oort, R.J., M.D. McCauley, S.S. Dixit, L. Pereira, Y. Yang, J.L. Respress, Q. Wang, A.C. De Almeida, D.G. Skapura, M.E. Anderson, et al. 2010. Ryanodine receptor phosphorylation by calcium/calmodulin-dependent protein kinase II promotes life-threatening ventricular arrhythmias in mice with heart failure. *Circulation.* 122:2669–2679. https://doi.org/10.1161/CIRCULATIONAHA.110.982298

Vassilakopoulou, V., B.L. Calver, A. Thanassoulas, K. Beck, H. Hu, L. Buntwal, A. Smith, M. Theodoridou, J. Kashir, L. Blayney, et al. 2015. Distinctive malfunctions of calmodulin mutations associated with heart RyR2-mediated arrhythmic disease. *Biochim. Biophys. Acta.* 1850:2168–2176. https://doi.org/10.1016/j.bbagen.2015.07.001

Voigt, N., N. Li, Q. Wang, W. Wang, A.W. Trafford, I. Abu-Taha, Q. Sun, T. Wieland, U. Ravens, S. Nattel, et al. 2012. Enhanced sarcoplasmic reticulum Ca^{2+} leak and increased Na^{+}-Ca^{2+} exchanger function underlie delayed afterdepolarizations in patients with chronic atrial fibrillation. *Circulation.* 125:2059–2070. https://doi.org/10.1161/CIRCULATIONAHA.111.067306

Vornanen, M., and N. Shepherd. 1997. Restitution of contractility in single ventricular myocytes of guinea pig heart. *Cardiovasc. Res.* 33:611–622. https://doi.org/10.1016/S0008-6363(96)00259-3

Wang, L., R.C. Myles, N.M. De Jesus, A.K. Ohlendorf, D.M. Bers, and C.M. Ripplinger. 2014. Optical mapping of sarcoplasmic reticulum Ca^{2+} in the intact heart: ryanodine receptor refractoriness during alternans and fibrillation. *Circ. Res.* 114:1410–1421. https://doi.org/10.1161/CIRCRESAHA.114.302505

Wehrens, X.H., S.E. Lehnart, S.R. Reiken, and A.R. Marks. 2004. Ca^{2+}/calmodulin-dependent protein kinase II phosphorylation regulates the cardiac ryanodine receptor. *Circ. Res.* 94:e61–e70. https://doi.org/10.1161/01.RES.0000125626.33738.E2

Xu, L., and G. Meissner. 2004. Mechanism of calmodulin inhibition of cardiac sarcoplasmic reticulum Ca^{2+} release channel (ryanodine receptor). *Biophys. J.* 86:797–804. https://doi.org/10.1016/S0006-3495(04)74155-7

You, Y., D.J. Pelzer, and S. Pelzer. 1997. Modulation of L-type Ca^{2+} current by fast and slow Ca^{2+} buffering in guinea pig ventricular cardiomyocytes. *Biophys. J.* 72:175–187. https://doi.org/10.1016/S0006-3495(97)78656-9

Yuan, W., and D.M. Bers. 1994. Ca-dependent facilitation of cardiac Ca current is due to Ca-calmodulin-dependent protein kinase. *Am. J. Physiol.* 267:H982–H993.

Zhang, L., J. Kelley, G. Schmeisser, Y.M. Kobayashi, and L.R. Jones. 1997. Complex formation between junctin, triadin, calsequestrin, and the ryanodine receptor. Proteins of the cardiac junctional sarcoplasmic reticulum membrane. *J. Biol. Chem.* 272:23389–23397. https://doi.org/10.1074/jbc.272.37.23389

Zhong, X., B. Sun, A. Vallmitjana, T. Mi, W. Guo, M. Ni, R. Wang, A. Guo, H.J. Duff, A.M. Gillis, et al. 2016. Suppression of ryanodine receptor function prolongs Ca^{2+} release refractoriness and promotes cardiac alternans in intact hearts. *Biochem. J.* 473:3951–3964. https://doi.org/10.1042/BCJ20160606

Zima, A.V., E. Picht, D.M. Bers, and L.A. Blatter. 2008. Termination of cardiac Ca^{2+} sparks: role of intra-SR [Ca^{2+}], release flux, and intra-SR Ca^{2+} diffusion. *Circ. Res.* 103:e105–e115. https://doi.org/10.1161/CIRCRESAHA.107.183236

Downloaded from http://rupress.org/jgp/article-pdf/152/11/e201912512/1801170/jgp_201912512.pdf by guest on 10 February 2026

Supplemental material

Measurements of [^{3}H]ryanodine binding in mouse ventricular homogenates

Preparation of tissue homogenates

Freshly dissected hearts were drained free of blood in Tyrode solution. The left ventricle was suspended in cold lysis buffer containing phosphatase and protease inhibitors (2 µM leupeptin, 100 µM PMSF, 500 µM benzamidine, 100 nM aprotinin, and 20 mM NaF) and homogenized using a Teflon pestle. The homogenized tissue was centrifuged at 1,000 *g* for 10 min at 4°C. Supernatants were aliquoted and stored at −80°C until used. The protein concentration was determined by the Bradford method.

[^{3}H]ryanodine binding assays

Binding assays were carried out following a modified version of a protocol previously described (Helms et al., 2016). Binding mixtures were prepared containing 75–100 µg of protein from the tissue homogenate, 0.2 M KCl, 40 mM Na-HEPES (pH 7.4), 5 nM [^{3}H]ryanodine (PerkinElmer), 1 mM EGTA, and enough $CaCl_2$ to set free [Ca^{2+}] in the range of 10 nM to 100 µM. The Ca^{2+}/EGTA ratio for these solutions was determined using MAXCHELATOR (https://somapp.ucdmc.ucdavis.edu/pharmacology/bers/maxchelator/). The binding reactions were incubated for 2 h at 37°C, then filtered through Whatman GF/B filters in an M24-R Harvester (Brandel). Nonspecific binding was determined in the presence of 20 µM ryanodine (MP Biomedicals). [^{3}H]ryanodine binding was measured by liquid scintillation.

Western blotting

Stored mouse ventricles were homogenized in 4 vol of lysis buffer (in mM): 20 sodium glycerolphosphate, 20 NaF, 1 EGTA, 2 EDTA, 0.2 Na_2VO_4, 2 dithiothreitol, 10 benzamide, 1 PMSF, 0.001 pepstatin, 1% IGEPAL, 0.01% Triton X-100, and 0.048 mg/ml leupeptin. Protein was measured by the Bradford method using BSA as a standard. Lysates (~90 µg of total protein) were separated per gel line in 10% SDS polyacrylamide gel (Mundiña-Weilenmann et al., 1996) and transferred to polyvinylidene difluoride membranes (Immobilon; MilliporeSigma). Blots were probed overnight with specific primary mAb at 4°C: RYR2 (1:1,000; Badrilla) and calsequestrin 2 (1:1,000; Invitrogen). The blots were then washed and incubated with secondary antibody (goat anti-rabbit and goat anti-mouse; Santa Cruz Biotechnology) for 2 h at room temperature. Immunoreactivity was visualized using a peroxidase-based chemiluminescence detection kit (Amersham Biosciences) with the ChemiDoc imaging system. The signal intensity of the bands in the immunoblots was quantified by densitometry using ImageJ software (National Institutes of Health).

Confocal imaging of intact cardiac myocytes

Freshly isolated mouse ventricular myocytes were loaded with 10 µM Fluo 3-AM (Molecular Probes) in Tyrode buffer containing 2.5 mM Ca^{2+} for 20 min at room temperature and mounted in a small chamber placed onto an inverted microscope equipped with a 63× lens objective as previously described (Palomeque et al., 2009). After stabilization (usually 3–5 min), confocal line scanning (512 × 512 pixels and 4.3 ms per line) was performed along the longitudinal axis of cells (avoiding nuclei) using the Zeiss LSM 410 confocal system in quiescent cells. The Fluo 3-AM–loaded myocytes were excited using the 488-nm argon laser, and the fluorescence emission was recorded at 500–550 nm. This procedure was repeated under high extracellular Ca^{2+} (6.0 mM Ca^{2+}) to induce SR Ca^{2+} overload. Cells were paced at 0.5 Hz for 30 s, and then pacing was stopped to register Ca^{2+} sparks. Ca^{2+} sparks were visually counted and expressed as the number of events per second, normalized to 100 µm (spark frequency).

Modeling

The modified ten Tusscher-Panfilov model (ten Tusscher et al., 2004) essentially consists of four Ca^{2+} compartments: cytosol, two dyadic clefts, and SR. Upon activation and L-type Ca^{2+} channel opening, Ca^{2+} is released from the SR by the CICR mechanism. This is described as Ca^{2+} release from the SR to the first cleft (DC1) through the RYR2 facing the L-type Ca^{2+} channels, and this Ca^{2+} then diffuses to the second cleft (DC2), inducing further CICR from the RYR2 not facing the L-type Ca^{2+} channel. Then, all the Ca^{2+} in DC2 either diffusing from DC1 or directly released to DC2 passes to cytosol, giving rise to the Ca^{2+} transient. Ca^{2+} release into DC1 and DC2 was based on the four-state Shannon model (Shannon et al., 2004) with open (O), rest (R), inhibited (I), and partially inhibited (IR) states, where the rate constants between them are governed by [Ca^{2+}] in the SR and Ca^{2+} release is given by:

$$Irelease = Vrel.O.\{([Ca^{2+}]_{SR}) - ([Ca^{2+}]_{DC})\},$$

where DC is DC1 or DC2 as appropriate. In addition, SR Ca^{2+} leak was represented as Ca^{2+} flow through the RYR2 modulated by the R state of this channel as follows:

$$Ileak = Vsp.R.\{([Ca^{2+}]_{SR}) - ([Ca^{2+}]_{DC})\},$$

Downloaded from http://rupress.org/jgp/article-pdf/152/11/e201912512/1801170/jgp_201912512.pdf by guest on 10 February 2026

resulting in total Ca^{2+} release through the RYR2 as follows:

Irel = Irelease + Ileak

(Lascano et al., 2013). Other model equations and parameter values were adopted from ten Tusscher and Panfilov (ten Tusscher et al., 2004; ten Tusscher and Panfilov, 2006).

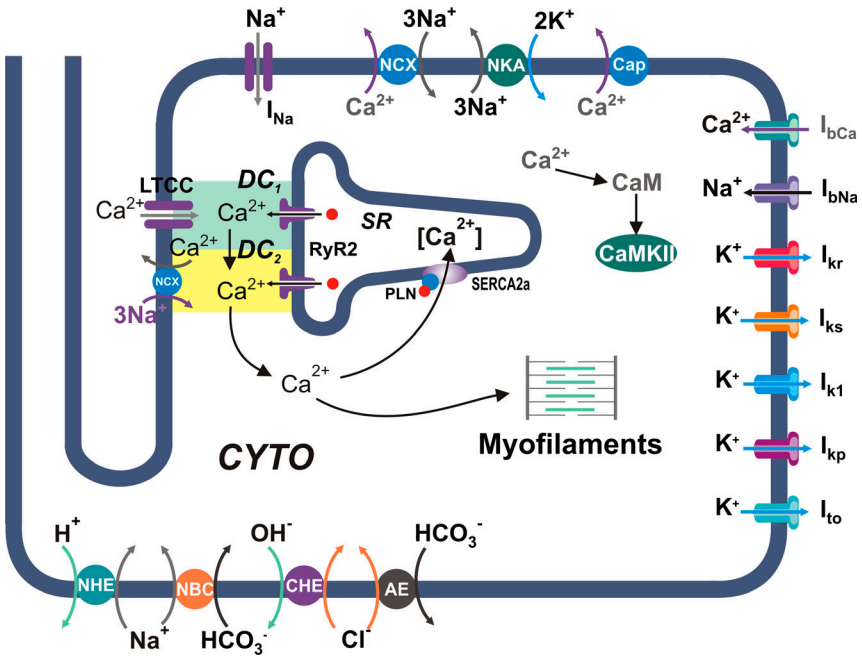

Figure S1. **Schematic diagram of the model.** Human myocyte model including ion pumps and exchangers responsible for action potential, Ca^{2+} management, force development, pH_i, and CaMKII regulation. Our previous model (Lascano et al., 2013) was modified by the addition of a second dyadic cleft: DC1 and DC2. The model is coupled to the myofilament force development model consisting of five-state troponin systems (TSs) with Ca^{2+} binding at the myofilament level (Negroni et al., 2015). AE, anion exchanger; Cap, membrane Ca^{2+}-ATPase; CHE, Cl^-/OH^- exchanger; CYTO, cytosol; LTCC, L-type Ca^{2+} channels; NBC, Na^+–$HCO3^-$ cotransporter; NCX, Na^+/Ca^{2+} exchanger; NHE, Na^+/H^+ exchanger; NKA, Na^+/K^+-ATPase.

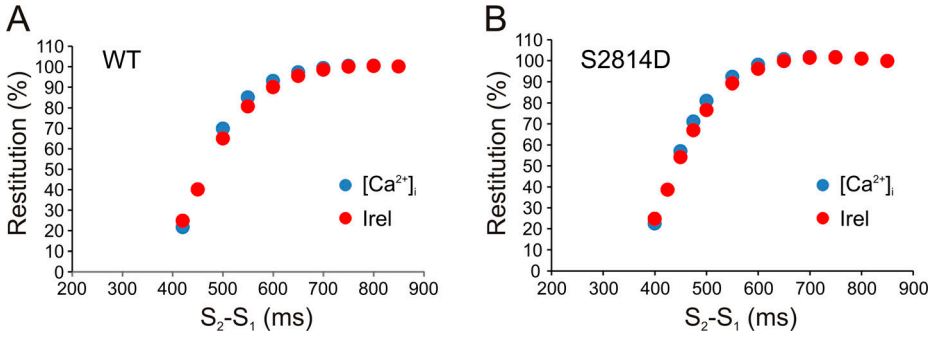

Figure S2. **Ca^{2+} transients or Irel restitution curves have a similar behavior in the human myocyte model. (A and B)** Cytosolic Ca^{2+} ($[Ca^{2+}]_i$) transient restitution (blue dots) and Irel restitution (red dots) have similar behaviors in the human myocyte model as shown for WT myocytes (A) and S2814D myocytes (B).

Downloaded from http://rupress.org/jgp/article-pdf/152/11/e201912512/1801170/jgp_201912512.pdf by guest on 10 February 2026

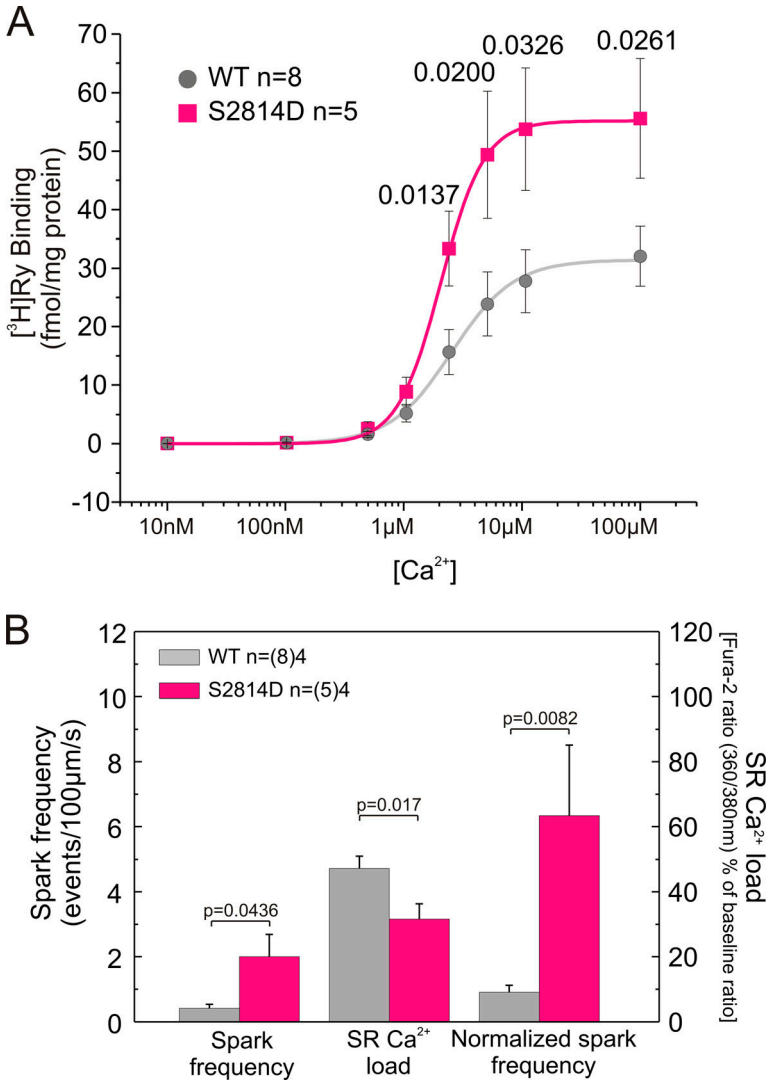

Figure S3. **S2814D mice show increased [³H]ryanodine binding and SR Ca^{2+} sparks frequency. (A and B)** Pseudophosphorylation of RYR2 at Ser2814 site (S2814D) significantly increases maximal density of high-affinity [³H]ryanodine binding sites (A) and the frequency of SR Ca^{2+} sparks (B). Data are expressed as mean ± SEM. n, number of animals. In B, numbers within parentheses are the number of cells.

Downloaded from http://rupress.org/jgp/article-pdf/152/11/e201912512/1801170/jgp_201912512.pdf by guest on 10 February 2026

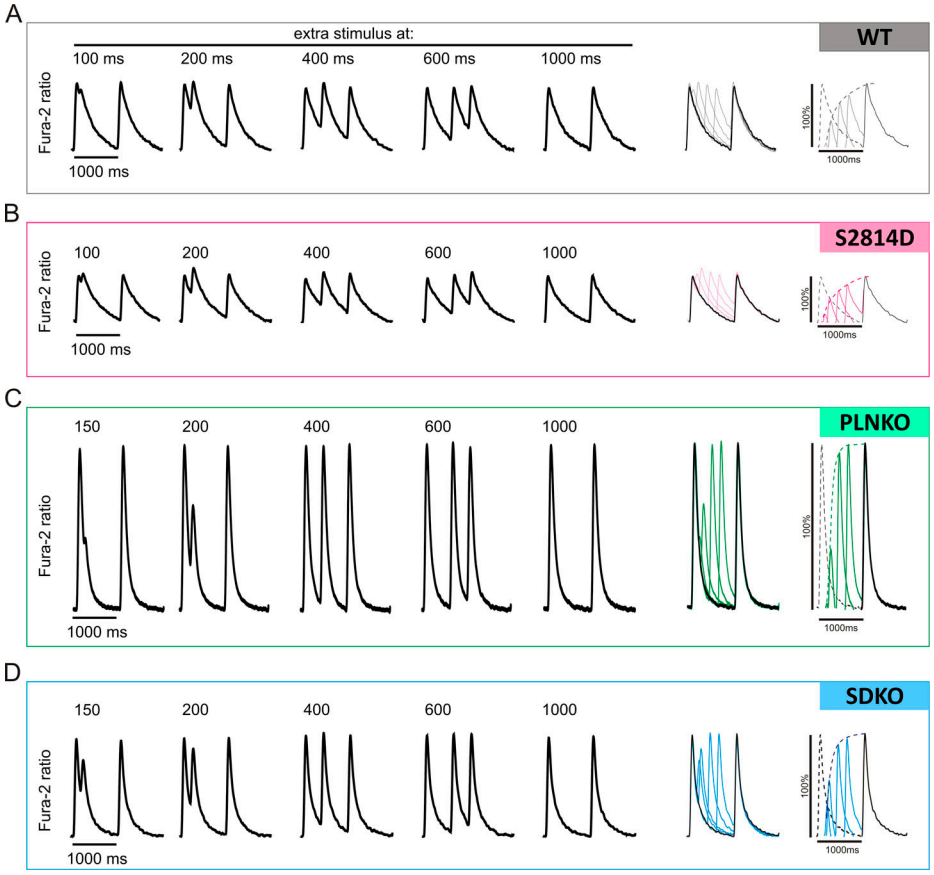

Figure S4. **Raw data of the experimental protocol used to determine CRR curves. (A–D)** Raw data of cytosolic Ca^{2+} measurements for WT (A), S2814D (B), PLNKO (C), and SDKO (D) myocytes used for CRR curves construction.

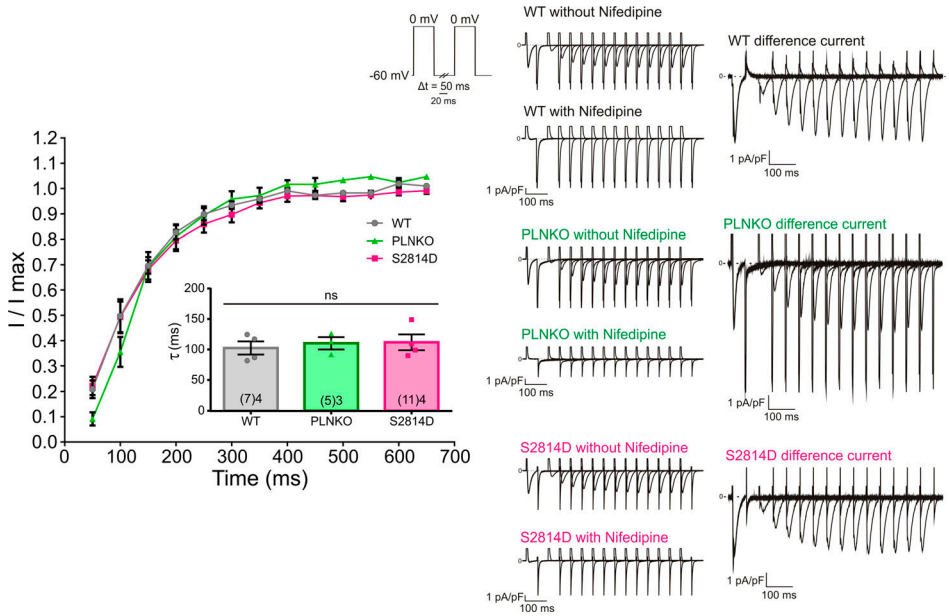

Figure S5. **ICaL restitution of WT, PLNKO, and S2814D recorded at 0 mV from a holding potential of −60 mV.** No changes were observed in the different strains. Right: Representative traces of the current evoked by the restitution protocol with the holding potential at −60 mV. The currents in the absence and presence of nifedipine and the nifedipine-sensitive current (difference current) are shown. The difference current was obtained by subtracting the current in the presence of nifedipine from the current recorded in its absence. Left: Average ICaL restitution determined in WT, PLNKO, and S2814D myocytes. The ICaL restitution time constants are shown in the inset. Data are expressed as mean ± SEM.

Downloaded from http://rupress.org/jgp/article-pdf/152/11/e201912512/1801170/jgp_201912512.pdf by guest on 10 February 2026

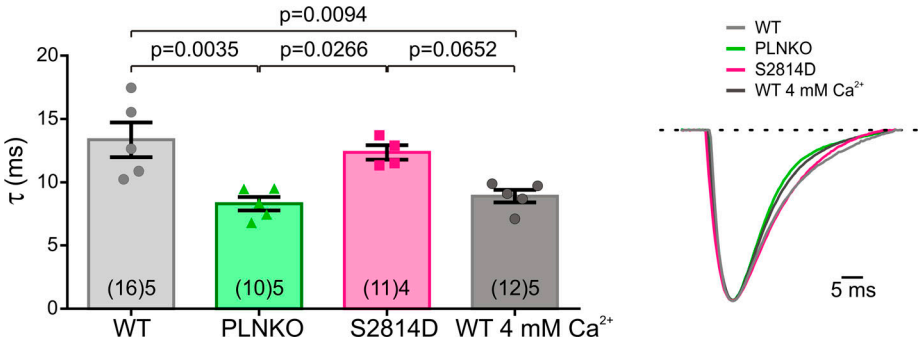

Figure S6. **The increase in extracellular Ca^{2+} and the ablation of PLN enhance ICaL inactivation kinetics.** Right: Representative traces of the current evoked by the first pulse to 0 mV of the restitution protocol recorded in myocytes of WT at 2 mM and 4 mM extracellular Ca^{2+} of PLNKO and of S2814D. Left: Average values of the time constants of inactivation of ICaL. Time constants were obtained after fitting the current traces from peak current to the end of the pulse with a monoexponential decay equation: $f(t) = \sum_{i=1}^{n} A_i e^{-t/\tau_i} + C$. Data are expressed as mean ± SEM.

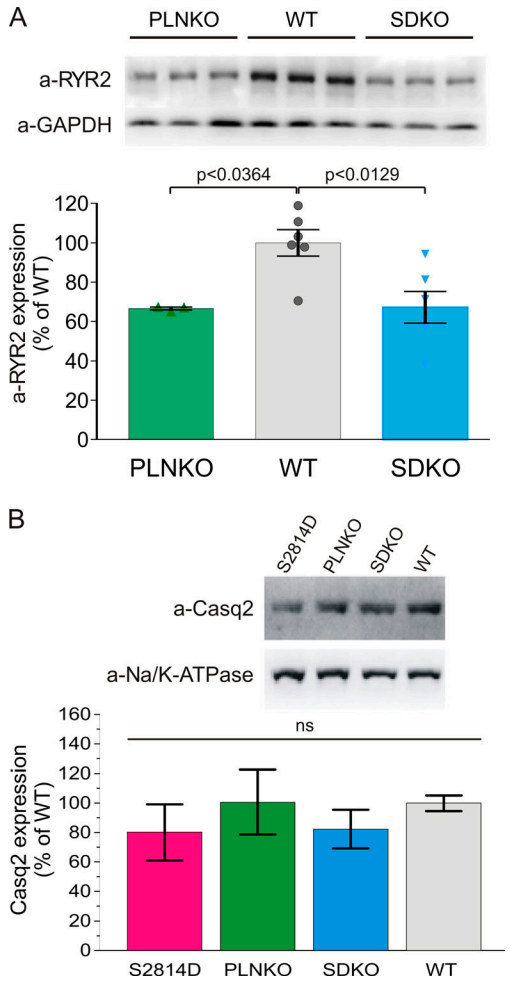

Figure S7. **Typical Western blots and overall results of RYR2 expression. (A)** Results confirm the previously described decrease of ∼30% in RYR2 expression in PLNKO and SDKO mice with respect to WT mice (Chu et al., 1998; Mazzocchi et al., 2016). Each bar represents mean data of six WT and SDKO hearts and three PLNKO hearts. **(B)** Casq2 expression does not significantly change in S2814D, PLNKO, and SDKO with respect to WT mouse hearts. Each bar represents mean data of five WT, S2814D, and SDKO hearts and four PLNKO hearts. Data are expressed as mean ± SEM.

Downloaded from http://rupress.org/jgp/article-pdf/152/11/e201912512/1801170/jgp_201912512.pdf by guest on 10 February 2026